

New specimens of *Allodaposuchus precedens* from France: intraspecific variability and the diversity of European Late Cretaceous eusuchians

JEREMY E. MARTIN^{1*}, MASSIMO DELFINO^{2,3}, GÉRALDINE GARCIA⁴,
PASCAL GODEFROIT⁵, STÉPHANE BERTON⁵ and XAVIER VALENTIN^{4,6}

¹Laboratoire de Géologie de Lyon: Terre, Planète, Environnement, UMR CNRS 5276 (CNRS, ENS, Université Lyon1), Ecole Normale Supérieure de Lyon, 69364 Lyon cedex 07, France

²Dipartimento di Scienze della Terra, Università di Torino, Via Valperga Caluso 35, Torino I-10125, Italy

³Institut Català de Paleontologia Miquel Crusafont, Universitat Autònoma de Barcelona, Edifici Z (ICTA-ICP), Carrer de les Columnes s/n, Campus de la UAB, E-08193 Cerdanyola del Valles, Barcelona, Spain

⁴Université de Poitiers, IPHEP, UMR CNRS 7262, 6 rue M. Brunet, 86073 Poitiers cedex 9, France

⁵Directorate 'Earth and History of Life', Royal Belgian Institute of Natural Sciences, rue Vautier 29, 1000 Brussels, Belgium

⁶Palaios Association, 86300 Valdivienne, France

Received 8 April 2015; revised 29 June 2015; accepted for publication 17 July 2015

A series of cranial remains as well as a few postcranial elements attributed to the basal eusuchian *Allodaposuchus precedens* are described from Velaux-La Bastide Neuve, a Late Cretaceous continental locality in southern France. Four skulls of different size represent an ontogenetic series and permit an evaluation of the morphological variability in this species. On this basis, recent proposals that different species of *Allodaposuchus* inhabited the European archipelago are questioned and *A. precedens* is recognized from other Late Cretaceous deposits of France and Romania. A dentary bone is described for the first time in *A. precedens* and provides a basis to reconsider the validity of two taxa, *Ischyrochamps meridionalis* and *Musturzabalsuchus buffetauti*, which are interpreted as possible junior synonyms of *Allodaposuchus*. These results allow the diversity of Late Cretaceous eusuchians from Europe to be refined and recognize a basal stock known as the Hylaeochampsidae sharing an absence of external mandibular fenestrae. Within this family, *Allodaposuchus* occupies a basal position relative to *Acynodon*, *Iharkutosuchus* and *Hylaeochampsia*.

© 2015 The Linnean Society of London, *Zoological Journal of the Linnean Society*, 2015

doi: 10.1111/zoj.12331

ADDITIONAL KEYWORDS: biogeography – Europe – Eusuchia – ontogeny.

INTRODUCTION

The endemic eusuchian crocodile *Allodaposuchus precedens* Nopcsa, 1928, from the Upper Cretaceous of Europe, was first revised on the basis of incom-

plete skull material from different localities in Spain, France and Romania (Buscalioni *et al.*, 2001) and has since attracted interest, partly because of its phylogenetic position as a basal eusuchian (Buscalioni *et al.*, 2001). In the last 10 years, relatively complete skulls from France, Romania and Spain became available, allowing for refinement of the morphology of *Allodaposuchus* (Martin & Buffetaut, 2005; Delfino *et al.*, 2008a; Martin,

*Corresponding author. E-mail: jeremy.martin@ens-lyon.fr

2010; Puértolas-Pascual, Canudo & Moreno-Azanza, 2013; Blanco *et al.*, 2014), but led to controversial scenarios about its phylogenetic relationships. Delfino *et al.* (2008a) confirmed the position of *Allodaposuchus* at the base of Eusuchia, but Martin (2010) placed this taxon as a member of Alligatoroidea. Most recent studies do not support this latter hypothesis. According to Puértolas-Pascual *et al.* (2013), *Allodaposuchus* is a member of Hylaeochampsidae, a basal eusuchian family including Early Cretaceous (*Hylaeochampsia vectiana*, *Pietraroiasuchus ormezzanoi*) and Late Cretaceous (*Iharkutosuchus makadii* and the genus *Acynodon*) representatives, exclusively from Europe (Buscalioni, Ortega & Vasse, 1997, 1999; Martin, 2007; Ósi, Clarck & Weishampel, 2007; Delfino, Martin & Buffetaut, 2008b; Rabi & Ósi, 2010; Turner & Brochu, 2010; Buscalioni *et al.*, 2011). However, the most recent analysis by Blanco *et al.* (2014) retrieved a position of *Allodaposuchus* somehow intermediate between the two previously proposed options. Under this new hypothesis *Allodaposuchus* is not recovered as a basal eusuchian and is not sitting in a derived position within Alligatoroidea. Blanco *et al.* (2014) recovered *Allodaposuchus* as part of the crown clade, outside the clade Brevirostres, when cranial and postcranial material is considered, or as part of a general polytomy at the base of the crown clade, when the analysis is based on skull elements only.

The diversity of Late Cretaceous eusuchians in continental deposits from Europe was recently reviewed by Martin & Delfino (2010), but the papers published in the last 5 years require the addition of one new genus (*Arenysuchus gascabadiolorum* Puértolas, Canudo & Cruzado-Caballero, 2011) and two new species of *Allodaposuchus* (*Allodaposuchus subjuniperus* Puértolas-Pascual *et al.*, 2013 and *Allodaposuchus palustris* Blanco *et al.*, 2014). Estimating past biodiversity is a challenging task when taxa of conservative morphology, such as freshwater eusuchians, are often recovered as isolated and/or fragmentary bones. The few cases in which more than a single fragmentary individual is present within a locality represent exceptional opportunities because it allows estimation of morphological trait variation in a geologically synchronous assemblage.

Here, we describe several *Allodaposuchus* specimens, represented by complete and fragmentary skull, mandibular and postcranial remains recovered from a bone accumulation at a single locality, interpreted as a freshwater deposit. These discoveries represent a unique opportunity to appreciate new morphological traits in *Allodaposuchus* in the frame of intraspecific and ontogenetic variabilities, to evaluate the synonymy of other crocodylomorph species, refine the phylogenetic affinities of *Allodaposuchus* and, finally, to provide an updated picture of crocodylomorph

diversity in the Late Cretaceous European archipelago.

GEOLOGICAL CONTEXT

The Velaux-La Bastide Neuve (VBN) site is located in the eastern part of the Aix-en-Provence Basin (Bouches du Rhône Department, southern France), close to the 'Étang de Berre' (Fig. 1). This fossil locality was discovered during a geological survey by one of us (X.V.) in 1992, in continental Late Cretaceous deposits (Valentin *et al.*, 2010). The outcrop consists of a 16-m-thick sequence of fluvial sandstones inserted within floodplain red clays and topped by a lacustrine limestone. Three main vertebrate fossil horizons were identified, containing an accumulation of well-preserved and slowly transported bones of numerous reptiles of different sizes. The eusuchian skull elements come from the principal rich concentration of bones (1 m thick) at the base of the stratigraphic section. Numerous isolated remains were also collected including teeth, vertebrae, osteoderms, and bones of the front and hind limbs.

Excavations (in 2009 and 2012) were conducted by the association Palaios and the Royal Belgian Institute of Natural History and were supported by the Conseil Général des Bouches du Rhône (CG 13 Department) and the Velaux Municipality. A diverse fauna was recovered, including bony fishes (Lepisosteidae; L. Cavin, pers. comm.), hybodont elasmobranchs (Meristonoides; G. Cuny, pers. comm.), pleurodiran and cryptodiran turtles (cf. genera *Solemys* and *Polysternon*) and pterosaurs. Dinosaurs are represented by the endemic ornithomimid *Rhabdodon*, Nodosauridae, Neoceratosauria, Dromaeosauridae and Titanosauria (the new genus *Astinganosaurus velauciensis* Garcia *et al.*, 2010). The vertebrate assemblage is associated with numerous charophytes (Porocharacea), reptilian eggshells (mainly megaloolithid and prismatic dinosaur types) and invertebrates (decapods, small gastropods and unionid bivalves).

The VBN section is situated about 10 km to the east and stratigraphically 15 m below the historical 'Lower Rognac Limestone Formation' ('Calcaire de la Gare de Rognac'). Along the section, the site has yielded *in situ* dinosaur clutches of *Megaloolithus aureliensis* and various isolated reptilian eggshells (testudoid, crocodiloid and prismatic morphotypes; G.G., pers. observ.), as well as ostracods and several species of charophytes (*Saportanella maslovi*, *Peckichara pectinata*, *Peckichara cancellata*, *Platychara caudata* and ?*Amblyochara begudiana*; M. Feist, pers. comm.). The co-occurrence of a charophyte association corresponding to the biozone chron 32n–32r (defined by Riveline, 1986; equating to 71.6–74 Ma, Gradstein *et al.*, 2012) and the dinosaur egg oospecies *Megaloolithus aureliensis* (following the

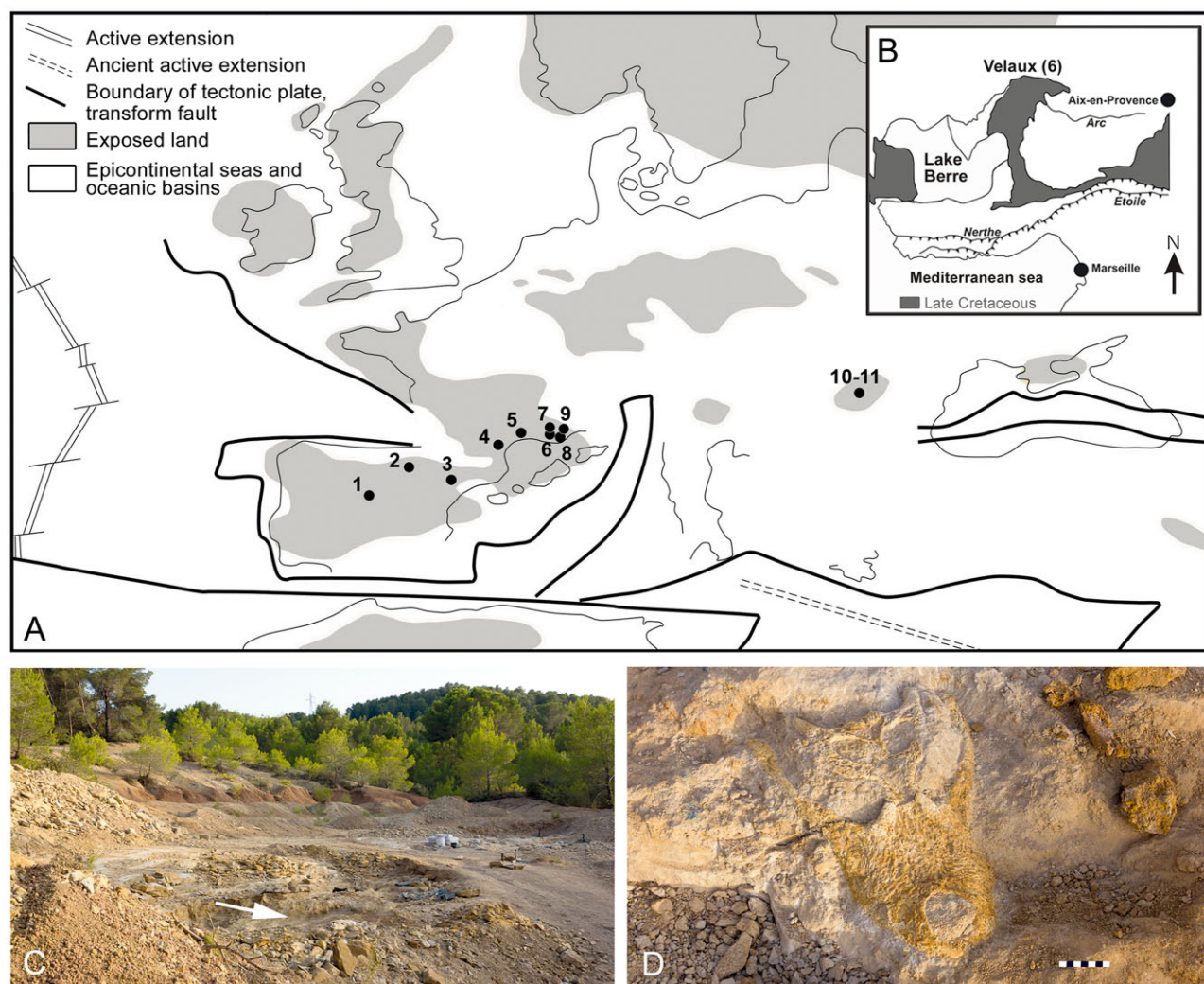


Figure 1. A, simplified palaeogeographical map of Europe and Peri-Tethyan area for the Late Cretaceous (Campano-Maastrichtian) (modified from Dercourt *et al.*, 2000). Location of contemporaneous sites with remains of the genus *Allodaposuchus*. 1, Armuña (Segovia, Spain); 2, Laño (Basque-Cantabrian region, Spain); 3, Vilamitjana (Catalonia, Spain); 4, Bellevue (Aude, France); 5, Cruzy (Hérault, France); 6, Velaux-La Bastide Neuve (Bouches du Rhône, France); 7, Saint Estève Janson (Bouches du Rhône, France); 8, Pourrières (Var, France); 9, Fox-Amphoux (Var, France); 10, Valioara (Transylvania, Romania); 11, Oarda de Jos (Transylvania, Romania). B, geographical location of the Velaux-La Bastide Neuve site with C, general view of the excavation and D, one of the skulls (MMS/VBN-12-10A) of *A. precedens* *in situ*. The white arrow indicates the fossiliferous level.

ostratigraphy of Garcia & Vianey-Liaud, 2001) clearly indicate a Late Campanian age for the VBN site.

Institutional abbreviations

MMS/VBN, Musée du Moulin seigneurial/Velaux-La Bastide Neuve; MFGI, Magyar Földtani és Geofizikai Intézet, Hungarian Geological and Geophysical Institute, Budapest; MCNA, Museo de Ciencias Naturales de Alava, Spain; MDE, Musée des Dinosaures, Espéraza, France; MNHN, Muséum National d'Histoire Naturelle,

Paris, France; PSMUBB, Paleontology-Stratigraphy Museum, University Babeş-Bolyai, Cluj-Napoca, Romania.

MATERIAL AND METHODS

ONTOGENETIC SCALING

To assess the ontogenetic variation of the *Allodaposuchus* skull, a linear regression was plotted on the basis of measurements of the seven complete skulls of *Allodaposuchus* from France, Romania and Spain

available from the literature (Supporting Information Appendix S1). Measurements taken are as follows: (1) skull length defined as the distance from the anterior tip of premaxilla to posterior edge of supraoccipital; and (2) skull width defined as the distance between the lateral edges of the quadrate condyles. Finally, the three complete skulls of *Acynodon* and the skull of *Arenysuchus* were also plotted in this space for comparison with a set of 13 individuals of the extant short-snouted *Osteolaemus* and five individuals of *Crocodylus niloticus*.

PHYLOGENETIC ANALYSIS

The specimens of *Allodaposuchus precedens* from MMS/VBN represent the most complete sample for this taxon and therefore it was re-coded in the character list established by Brochu *et al.* (2012). *Allodaposuchus subjuniperus* was not considered in this study due to its controversial status (see Discussion) and previous codings of *A. precedens* specimens from other European localities were dismissed because they are not as complete as the material from MMS/VBN. The scores of the two species of *Acynodon* known from complete skulls, *A. iberoccitanus* and *A. adriaticus* (Martin, 2007; Delfino *et al.*, 2008b), were double-checked (all scores are provided in Supporting Information Appendix S2). A total of 96 taxa were analysed using the software TNT (Goloboff, Farris & Nixon, 2003), including *Bernissartia fagesii* as the outgroup taxon, which was coded for 179 characters. The results are provided in Figure 13. Bremer's decay index was used to assess the robustness of the resulting consensus cladogram.

SYSTEMATIC PALAEONTOLOGY

ORDER CROCODILIA GMELIN, 1789

SUBORDER EUSUCHIA HUXLEY, 1875

FAMILY HYLAECHAMPSIDAE ANDREWS, 1913

GENUS *ALLODAPOSUCHUS* NOPCSA, 1928

ALLODAPOSUCHUS PRECEDENS NOPCSA, 1928 (SEE FIGS 2–10)

Referred specimens: MMS/VBN-12-42, a nearly complete skull of a juvenile; MMS/VBN-12-10A, a complete adult skull; MMS/VBN-12-10B, a right dentary associated with the large adult skull MMS/VBN-12-10A; MMS/VBN-93-28, a dorsoventrally compressed subadult skull; MMS/VBN-12-10D, a juvenile skull table; MMS/VBN-93-29, isolated fragmentary left maxilla; MMS/VBN-93-30, isolated fragmentary right maxilla possibly corresponding to MMS/VBN-93-29; MMS/VBN-12-10F, one dorsal osteoderm; MMS/VBN-02-37, a left femur.

Occurrence: Late Campanian fluvial deposits of Velaux-La Bastide Neuve, Bouches du Rhône Department, southern France.

Emended diagnosis: *Allodaposuchus precedens* is a hylaeochampsid crocodilian characterized by the following combination of characters: mesorostrine skull; external naris large and rostr dorsally orientated; ectopterygoid bordering the posterior tooth row margin; laterally open canalis quadratosquamosoexoccipitalis; participation of the nasals in the posterior portion of the external naris; largest maxillary alveolus in fourth position; 13 maxillary alveoli. *Allodaposuchus precedens* differs from *Acynodon*, *Hylaeochampsia* and *Iharkutosuchus* by having a mesorostrine skull, and from *Acynodon* and *Iharkutosuchus* by having an enlarged fourth maxillary alveolus and conical pointed teeth. *Allodaposuchus precedens* differs from *A. iberoccitanus* by lacking a preorbital ridge, and from *I. makadii* by lacking multicusped posterior maxillary teeth and by having open supratemporal fenestrae.

DESCRIPTION

Preservation, form and general features: The skull MMS/VBN-12-42 (Fig. 2) is nearly complete, but the anterior region is slightly compressed in the posterior direction and the right lateral surface of the premaxilla and the maxilla is absent up to the fourth maxillary alveolus. The right quadrate is mostly missing and the left quadrate condyle has been eroded. The pterygoids are only partly preserved (the internal choana is absent). The posteroventral tip of the ectopterygoid is broken off. In dorsal view, the rostrum is relatively elongated (Supporting Information Appendix S1), with just a hint of a premaxillary–maxillary notch on the left side (the right side is damaged). In lateral view, the ventral edge of the skull is markedly undulated, with the apex of the convexities corresponding to the middle of the premaxilla, the fourth and the tenth maxillary alveoli, and the bottom of the concavities corresponding to the premaxilla–maxilla suture and the sixth interalveolar space. The skull MMS/VBN-12-10A (Figs 3, 4) is complete and experienced little deformation, only detectable by a slight dorsoventral compression of the occipital condyle (Fig. 5). One main fracture is transversally orientated through the skull at the level of the interorbital area and reaches the fourth maxillary alveolus on the left side. On the ventral surface, this fracture extends from the anterior edge of the fourth maxillary left alveolus to the anterior edge of the eleventh right maxillary alveolus. The right premaxilla is bent inward as shown by the orientation of the teeth. The left tooth row is deformed and deflected to the outer side of the skull, as indicated by the shift of the row away from the foramina located medially (Fig. 4). The third skull, MMS/VBN-93-28 (Fig. 6), is less complete and is missing much of the palate, the temporal regions and several zones of the skull table. It is comparable in size to MMS/VBN-12-42, but experienced some dorsoventral

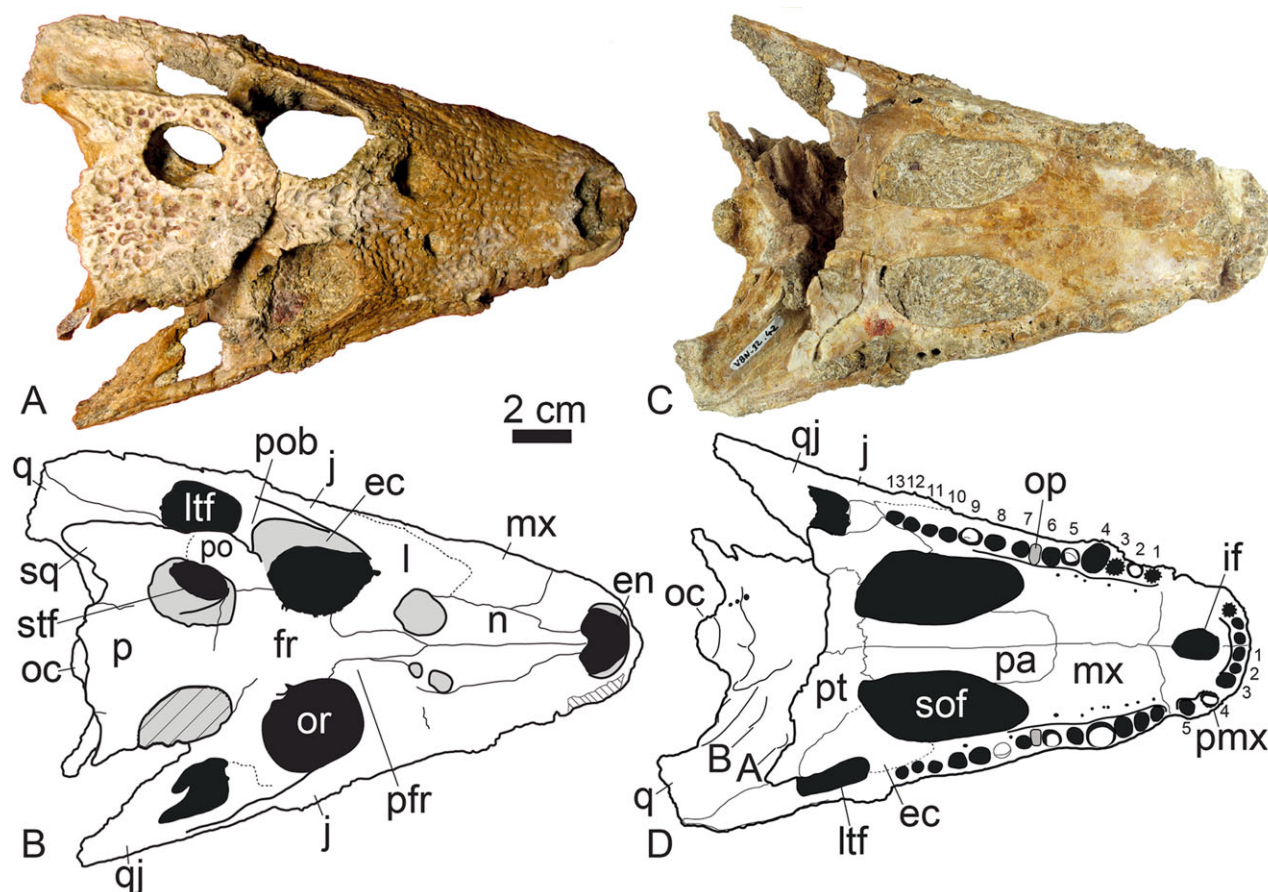


Figure 2. The juvenile skull of *Allodaposuchus precedens* Nopcsa, 1928 (MMS/VBN-12-42) from the Campanian of Velaux-La Bastide Neuve, France in dorsal (A, B) and ventral views (C, D) with photographs and associated line drawings. Abbreviations: ec, ectopterygoid; en, external nares; fr, frontal; if, incisive foramen; j, jugal; ltf, lower temporal fenestra; l, lacrimal; mx, maxilla; n, nasal; oc, occipital condyle; or, orbit; p, parietal; pa, palatine; pfr, prefrontal; pmx, premaxilla; po, postorbital; pob, postorbital bar; pt, pterygoid; q, quadrate; qj, quadratojugal; sof, suborbital fenestra; sq, squamosal; stf, supratemporal fenestra. Numbers denote alveolar positions.

compression, resulting in a broader outline of the rostrum. The fourth skull, MMS/VBN-12-10D (Fig. 7), consists of a skull table and quadrate branch, preserving details of the otic area and of the supratemporal fenestrae. In the large specimen MMS/VBN-12-10A the skull table is concave not only because the rims of the supratemporal fenestra are slightly raised, but because the areas anterior and posterior to the fenestrae are distinctly depressed. The interfenestral space is less than half the interorbital space. The posterior surface of the rostrum of MMS/VBN-12-42 is affected by three circular holes of different sizes, the largest being more than 1 cm in diameter. The origin of these holes is uncertain, but could be post-mortem as there is no sign of reaction tissue formed during healing.

Ornamentation: MMS/VBN-12-10A has deep irregular pits in the skull table and interorbital dorsal surface.

These pits are numerous, but shallow on the rostrum and they become circular and more spaced above the maxillary tooth row. The pits become deeper and vermiform along the infratemporal bar. The quadratojugal is dorsally inflated with pits that do not spread over its medial area. Anterior to the orbits, the thick orbital bulge has a very small pitted surface. The lateral side of the squamosal is pierced with large foramina. Pits on the postorbital are similar to the anterior orbital rim. On the dorsal surface of the squamosal, there is a large depression, as in *Rugosuchus nonganensis* (Wu, Brinkman & Fox, 2001).

CRANIAL OPENINGS

External nares: The confluent external naris is wider than long, but it is possible that its length was affected by the preservation of the anterior region of the

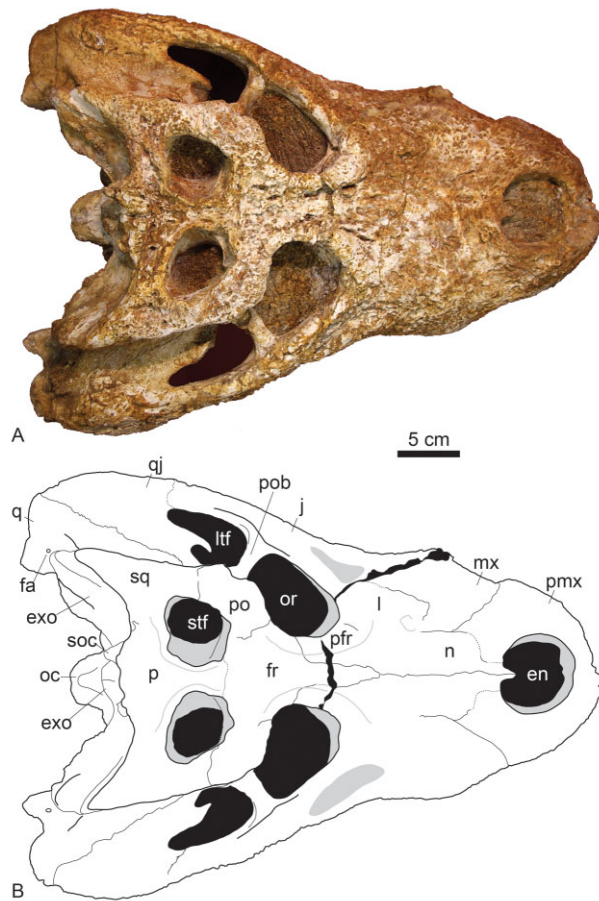


Figure 3. An adult skull of *Allodaposuchus precedens* Nopcsa, 1928 (MMS/VBN-12-10A) from the Campanian of Velaux-La Bastide Neuve, France in dorsal view: A, photograph and B, associated line drawing. Abbreviations: bo, basioccipital; en, external nares; exo, exoccipital; fa, foramen aëreum; fr, frontal; j, jugal; l, lacrimal; ltf, lower temporal fenestra; mx, maxilla; n, nasal; or, orbit; p, parietal; pfr, prefrontal; pmx, premaxilla; po, postorbital; pob, postorbital bar; q, quadrate; qj, quadratojugal; soc, supraoccipital; sq, squamosal; stf, supratemporal fenestra.

skull. The narial rim is not significantly elevated, but is slightly orientated anterodorsally (Fig. 8).

Orbits: In MMS/VBN-12-10A, the largest available specimen, the medial and anterior rims of the orbits are greatly thickened and dorsally raised. In the smaller specimen MMS/VBN-12-42, the orbital rims are slightly raised, but are thin. In both skulls, there is no interorbital ridge. In MMS/VBN-12-10A, the lacrimal hosts a foramen visible on the orbital wall of the left side. It opens at the lateral edge of the prefrontal lamina. The interorbital space is moderately concave because the orbital rim is slightly raised medially despite being thin. The orbital rim is thin and sharp on its

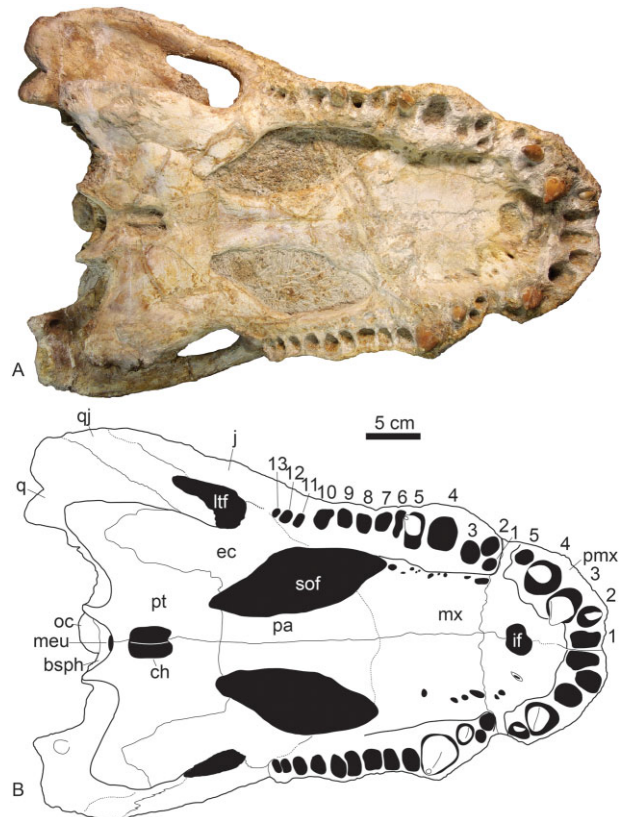


Figure 4. An adult skull of *Allodaposuchus precedens* Nopcsa, 1928 (MMS/VBN-12-10A) from the Campanian of Velaux-La Bastide Neuve, France in ventral view: A, photograph and B, associated line drawing. Abbreviations: bsph, basisphenoid; ch, choanae; ec, ectopterygoid; if, incisive foramen; j, jugal; ltf, lower temporal fenestra; me, median Eustachian opening; mx, maxilla; oc, occipital condyle; pa, palatine; pmx, premaxilla; pt, pterygoid; q, quadrate; qj, quadratojugal; sof, suborbital fenestra. Numbers denote alveolar positions.

lateral margin, but is flush with the surface of the rostrum on its anterior margin.

Supratemporal fenestrae: The bones of the skull table do not significantly overhang the supratemporal fenestrae in MMS/VBN-12-42 and MMS/VBN-12-10A. A shelf is clearly present at the anteromedial corner of the left fenestra (the condition of the right fenestra is not visible) where it extends both medially (along the anterior wall of the fossa) and posteriorly (along the medial wall of the fossa). Such a shelf is clearly present in both fenestrae of MMS/VBN-12-10A, in which it is less developed posteriorly. In the latter specimen, a sharp, cutting ridge marks the posterolateral surface of the shelf. In MMS/VBN-12-42, the skull table is flat and the rim around the medial margin of the supratemporal fenestra is slightly elevated; the

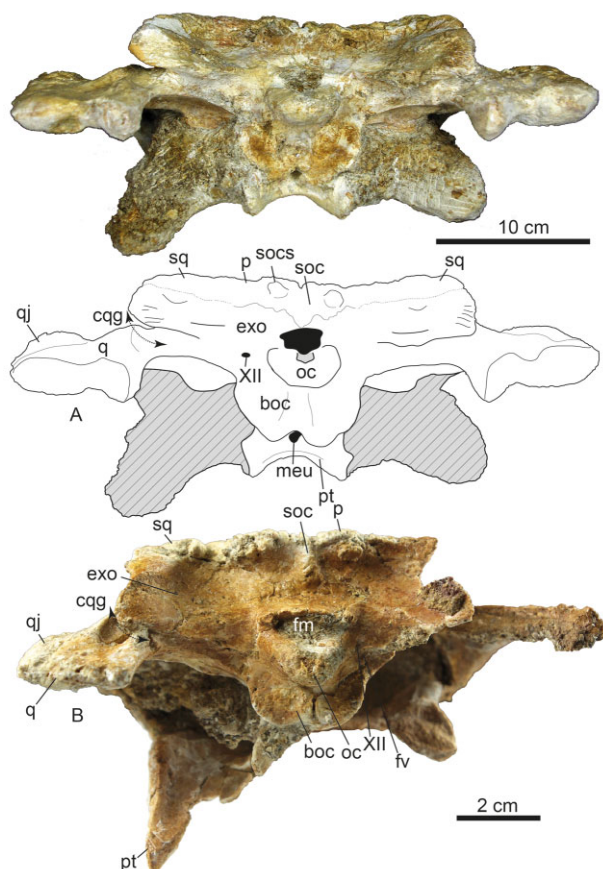


Figure 5. Posterior views of adult (A, MMS/VBN-12-10A; B, associated line drawing) and juvenile (C, MMS/VBN-12-42) specimens of *Allodaposuchus precedens* Nopcsa, 1928 from the Campanian of Velaux-La Bastide Neuve, France. Abbreviations: boc, basioccipital; cqg, cranioquadrate groove; exo, exoccipital; fm, foramen magnum; fv, foramen vagus; meu, median Eustachian foramen; oc, occipital condyle; p, parietal; pt, pterygoid; q, quadrate; qj, quadratojugal; soc, supraoccipital; socs, supraoccipital spine; sq, squamosal; XII, foramen for cranial nerve XII. Oblique hatching denotes sediment.

interfenestral space is approximately as wide as the supratemporal fenestra. The interfenestral and interorbital spaces have approximately the same width.

Orbitotemporal foramen: In MMS/VBN-12-10A, the orbitotemporal foramina are visible in dorsal view, but their sutures cannot be assessed. In MMS/VBN-12-10D (Fig. 7), the orbitotemporal foramen is small (4 mm wide), slit-like and opens on the posterior wall of the supratemporal fossa. Its ventral margin is built mostly by the medial projection of the squamosal, which contacts the parietal near the medial corner of the orbitotemporal foramen. Thus, the parietal and

squamosal do exclude the quadrate from the ventral margin of the orbitotemporal foramen.

Infratemporal fenestrae: In both MMS/VBN-12-42 and MMS/VBN-12-10A, the infratemporal fenestrae are smaller than the orbits, nearly as long as wide, and open along the anterior half of the skull table. A long and robust quadratojugal spine penetrates this fenestra (Figs 2, 3).

Suborbital fenestrae: The suborbital fenestrae are longer than wide and have more rounded anterior and posterior angles in the smaller specimen MMS/VBN-12-42 than in MMS/VBN-12-10A. In MMS/VBN-12-10A, the posterior angle is narrow and makes an incision into the pterygoid. In both MMS/VBN-12-42 and MMS/VBN-12-10A, the suborbital fenestrae extend anteriorly up to the seventh interalveolar space (Figs 2, 4).

Choanae: In MMS/VBN-12-10A, the internal choana is subrectangular, longer than broad, septate and placed close to the posterior edge of the pterygoids. It is not clear if the septum was recessed into the choana or if it projected out of it. Around the choana, there is a weak depression that therefore does not give origin to a clear neck. The orientation of the choana is fully ventral as preserved, contradicting with the posteroventrally orientated choana in, for example, *C. niloticus*. It is assumed here that a slight deformation of the area altered the original anteroventral orientation (compare directions of pterygoid wings in Fig. 8).

SKULL

Premaxilla: The premaxilla is preserved in the three nearly complete skulls, but it is incomplete in MMS/VBN-93-28. On the dorsal surface of the rostrum, the posterior processes of the premaxillae reach the level of the third maxillary alveolus or the third interalveolar space. On the palatal surface, the premaxilla–maxilla suture is transversely orientated and is found in the space occupied by the first maxillary alveolus. In lateral view, the premaxilla is separated from the maxilla by a notch (Fig. 8). This emargination sits in a lateral position to the premaxilla, allowing the laterally occluding dentary ‘canine’ to be visible in lateral and dorsal views. The total number of premaxillary alveoli is five as indicated by MMS/VBN-12-40 and MMS/VBN-12-10A. The posterior premaxillary tooth row of the juvenile MMS/VBN-12-42 is damaged on both sides, but the right one shows the following sequence (Supporting Information Appendix S1): two subequal alveoli, followed by a larger one, then a tooth in position, then a last alveolus. All alveoli are approximately circular in outline. In MMS/VBN-12-10A, the first premaxillary

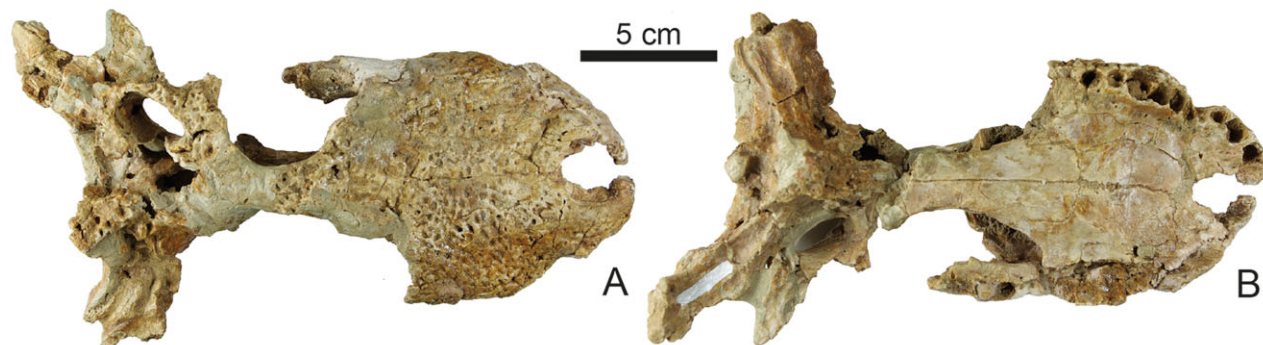


Figure 6. Skull of *Allodaposuchus precedens* Nopcsa, 1928 (MMS/VBN-93-28) from the Campanien of Velaux-La Bastide Neuve, France in A, dorsal and B, ventral views.

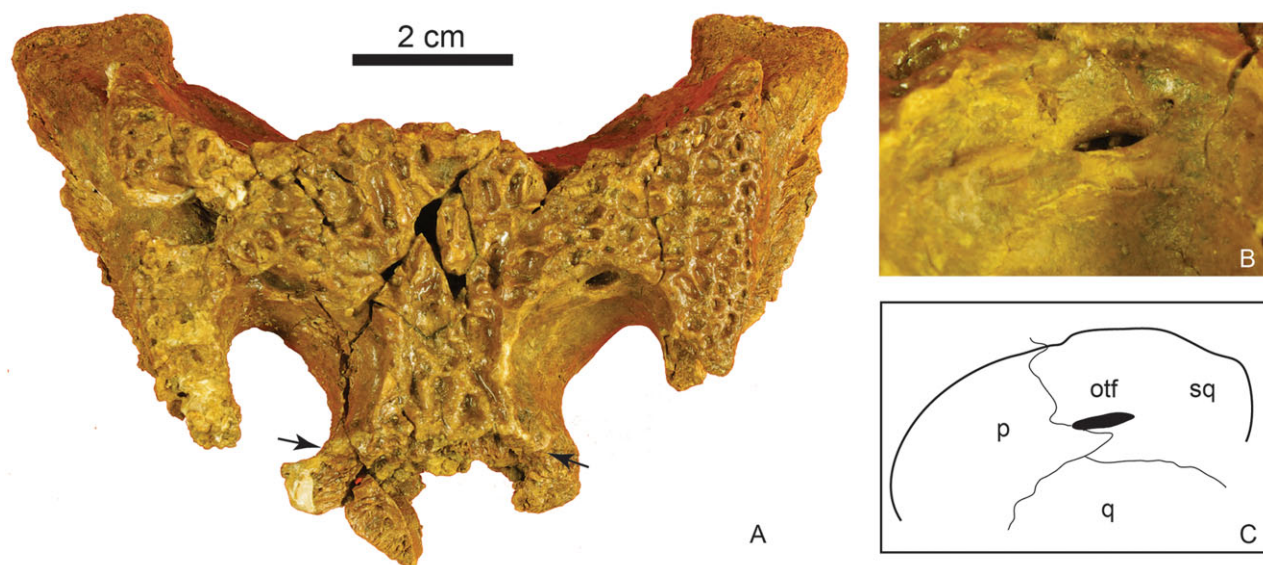


Figure 7. The skull table of a juvenile *Allodaposuchus precedens* Nopcsa, 1928 (MMS/VBN-12-10D) in A, dorsal view and details of the left supratemporal fenestra in anterior view (B) with interpretive line drawing (C) of the sutures around the orbitotemporal foramen. Abbreviations: otf, orbitotemporal foramen; p, parietal; q, quadrate; sq, squamosal. Arrows indicate the position of the frontoparietal suture.

depression can be interpreted either as an alveolus, an occlusal pit or a combination of both. This structure is labiolingually expanded. Assuming that there are five premaxillary alveoli, the fourth is the largest and teeth are preserved in alveoli 2–4 on the right side and 4–5 on the left side. Alternatively, the first depression might be considered as an occlusal pit and in that case there are only four premaxillary alveoli, the third of which is the largest. The premaxillary tooth row is distinctly lowered relative to the palatal surface. In MMS/VBN-12-10A, the incisive foramen is relatively small, circular and located far from the premaxillary–maxillary suture. It spreads between the last two alveoli, almost at the level of the premaxillary–maxillary notch. On the other hand, in MMS/VBN-

12-42, the incisive foramen is also located far from the suture, but is comparatively larger and is ovoid, spreading between the third and last premaxillary alveoli.

Maxilla: The maxilla is described from specimens of small (MMS/VBN-12-42), intermediate (MMS/VBN-93-28) and large (MMS/VBN-12-10A) sizes. On the dorsal surface, the maxillae are separated medially by the nasals and the premaxillae. The tooth row is undulated in lateral view and projects ventrally to the palatal surface from maxillary alveolus 1 to 7. Posteriorly, the tooth row is at the same level as the rest of the palate. On the palatal surface of the maxillae, the maxillary foramen for the cranial nerve V is rather small (much smaller than one alveolus) and opens close

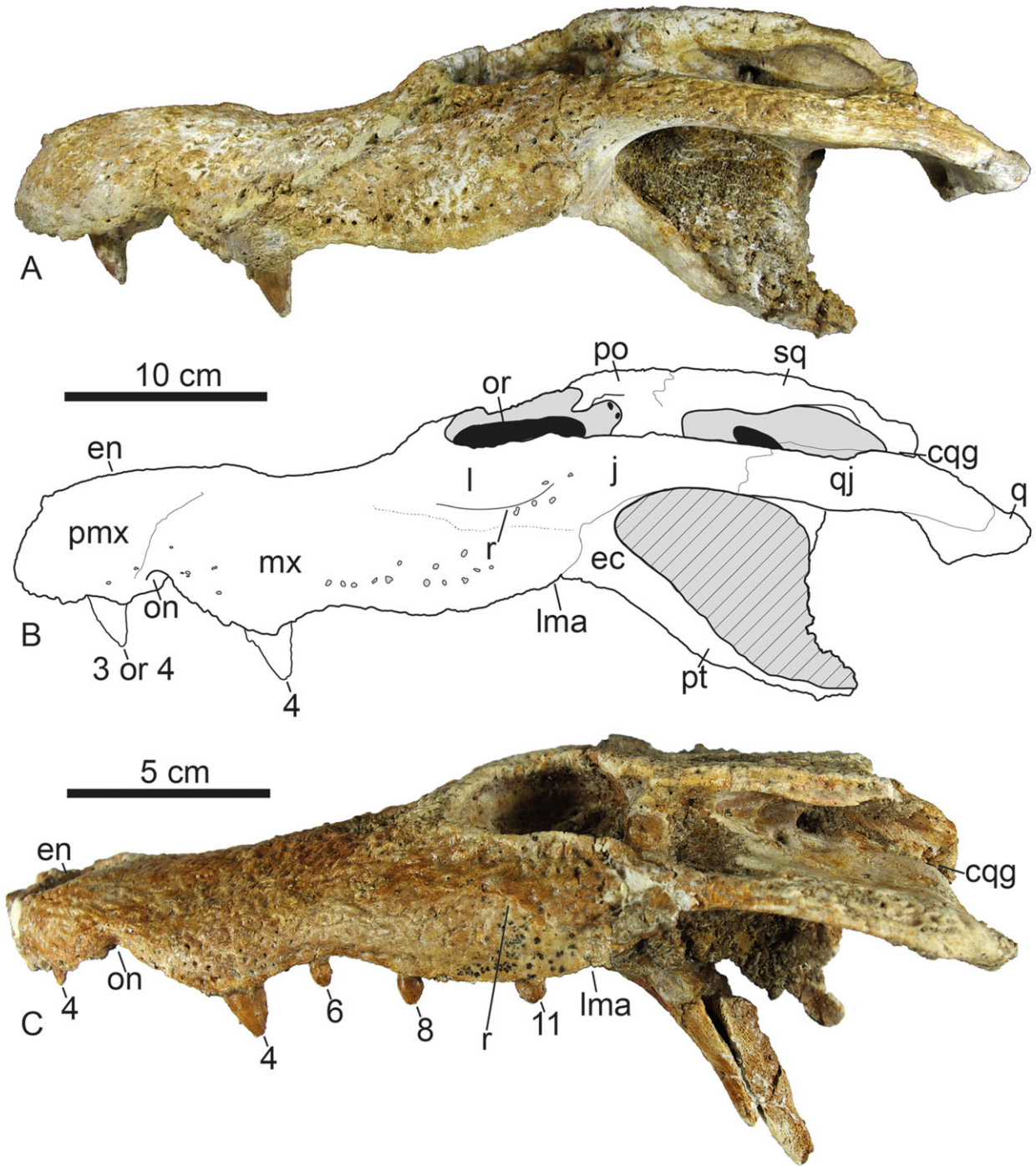


Figure 8. Left lateral views of adult (A, MMS/VBN-12-10A; B, line drawing) and juvenile (C, MMS/VBN-12-42) specimens of *Allodaposuchus precedens* Nopcsa, 1928 from the Campanian of Velaux-La Bastide Neuve, France. Abbreviations: cqg, cranioquadrate groove; ec, ectopterygoid; en, external nares; lma, last maxillary alveolus; mx, maxilla; on, occlusal notch; or, orbit; pmx, premaxilla; po, postorbital; pt, pterygoid; q, quadrate; qj, quadratojugal; sq, squamosal. Numbers denote tooth positions. Oblique hatching denotes sediment.

to the anterior edge of the sixth alveolus. A series of relatively large foramina are located parallel to the tooth row, on the palatal surface, but close to the wall of the ventrally projecting tooth row. The foramen for the palatal ramus of the trigeminal nerve is not clearly distinguishable from the other foramina and therefore it cannot be considered as large as the alveoli. The posterior end of the maxillary tooth row terminates at mid-orbit level. Here, the external maxillary surface forms a vertical wall. Above this wall, an anteroposteriorly elongated outgrowth or ridge of the jugal overhangs the maxilla. There are 13 maxillary alveoli on both sides of MMS/VBN-12-42 and MMS/VBN-12-10A. The largest maxillary alveolus is the fourth. In both skulls, the size of the alveoli decreases posteriorly, although alveoli 8 and 9 seem to be slightly enlarged. The maxillary tooth row is approximately rectilinear. In MMS/VBN-12-10A, the first three maxillary alveoli on both sides of the skull have an unusual triangular arrangement, interpreted here as a pathology of growth (Fig. 3). Two isolated maxillae might belong to a single individual. The maxilla MMS/VBN-93-29 is heavily fractured, but the general shape is preserved. Part of the dorsal surface, palatal surface and the whole posterior region are missing. The preserved portion of this maxilla corresponds to the first ten alveoli. None of the alveoli hosts teeth. The shape of the alveoli is not circular, probably because of some degree of mediolateral deformation. The fourth alveolus is the largest. The alveoli anterior to the sub-orbital fenestra do not open at the level of the palatal surface, but much below it, thanks to a ventral protrusion of the entire tooth row. The right maxilla MMS/VBN-93-30 preserves the alveoli from 6 to 11 and the morphology is nearly the same as that of the left maxilla.

Nasal: In all specimens, the nasals are relatively broad and nearly parallel to each other for most of their length, but do suddenly shrink in the proximity of the external nares. This sudden shrink is more accentuated in the large specimen MMS/VBN-12-10A, whereas it is more progressive in the smaller specimen MMS/VBN-12-42. The nasals form about one-third of the posterior narial border and send a modest bar into the naris. Posteriorly, a short process of the frontal medially separates the nasals. The relationships of the nasals with the lacrimal and prefrontal are masked by the ornamentation in MMS/VBN-12-10A and by circular depressions, which probably occurred at death or post-mortem in MMS/VBN-12-42.

Lacrimal and prefrontal: Although these bones are preserved in MMS/VBN-12-10A and MMS/VBN-12-42, not much can be said due to the lack of visibility of the sutures. Both the lacrimal and the prefrontal partici-

pate in the anteromedial corner of the orbits. In MMS/VBN-12-10A, the prefrontal orbital margin consists of a prominent dorsally projecting bulge, attaining its maximal size near the prefrontal–lacrimal contact. This bulge continues on the medial side of the lacrimal. The lacrimal orbital margin is perfectly circular. As observed on the left side of MMS/VBN-12-10A, the lacrimal appears longer than the prefrontal and projects beyond the level of the anterior frontal process, i.e. well in front of the orbits at about mid-rostrum length. In MMS/VBN-12-42, a small lacrimal foramen is visible on the right side at the anterior corner of the right orbit. In MMS/VBN-12-10A, where it is best preserved, the internal wall of the left prefrontal has a laminar structure fitting exactly the description given by Delfino *et al.* (2008a) for the *A. precedens* skull from Romania.

Jugal: In MMS/VBN-12-10A, the jugal hosts a remarkably large foramen (1.1 cm in diameter) opening posteriorly, at the base of the postorbital bar (Fig. 9E). The jugal builds most of the large infratemporal bar, which is massive and circular in cross-section unlike for example in *Crocodylus*, where it is laminar. The jugal does not project beyond the posterior level of the lower temporal fenestra (Fig. 3). In ventral view, the lateral margin of the jugal seems to project far posteriorly, but the suture with the quadratojugal is not clearly discernible. The anterior part of the jugal forms the anterolateral margin of the orbits, but the lacrimal contact cannot be discerned. In the anterior end of the jugal, the bone is raised as a thick, approximately 7-cm-long ridge (Fig. 5), parallel to the infratemporal bar and protruding above the posterior part of the maxillary tooth row. An elongated depression is located between this ridge and the orbital rim. The jugal ridge overhangs substantially the posterior end of the maxilla. The jugal forms the base of the relatively slender postorbital bar, which is devoid of ornamentation and inset from the lateral surface of the bone.

Frontal: The frontal is complete in MMS/VBN-12-10A and MMS/VBN-12-42. Its anterior region can be guessed in MMS/VBN-93-28. The frontal separates the prefrontal medially and wedges between the posterior ends of the nasals. The frontal process extends beyond the anterior end of the orbits. The dorsal surface of the frontal is slightly concave in MMS/VBN-12-42, but this concavity is more expressed in MMS/VBN-12-10A, with a marked development of the periorbital bulges. The frontal makes the posteromedial corner of the orbits. Posteriorly, it slightly penetrates between the supratemporal fenestrae, as indicated by the linear frontoparietal suture preserved in MMS/VBN-12-10D (Fig. 7). It separates the parietal and postorbital to meet on the dorsal surface of the skull table. The frontal

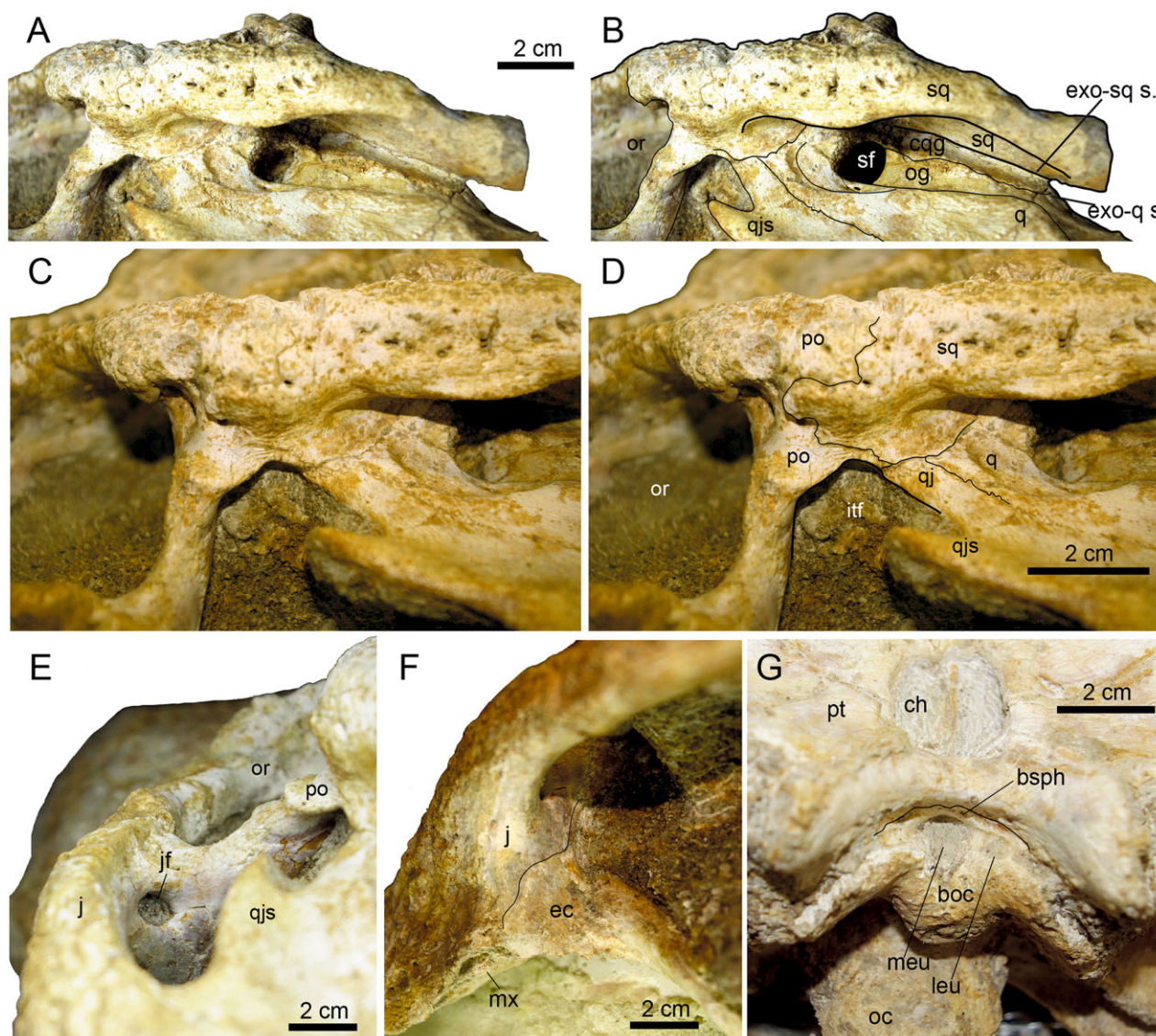


Figure 9. Details of the cranial anatomy of *Allodaposuchus precedens* Nopcsa, 1928 (MMS/VBN-12-10A) from the Campanian of Velaux-La Bastide Neuve, France: lateral view of the left otic area A, without and B, with underlined arrangement of the cranioquadrate groove; lateral view of the left postorbital pillar C, with and D, without sutural line drawings; E, posterior view through the left lower temporal fenestra showing the large jugal foramen; F, posteroventral view of the left temporal arch showing the dorsal extent of the ectopterygoid on the postorbital pillar; G, posteroventral view of the basisphenoid showing the median Eustachian foramen. Abbreviations: boc, basioccipital; bsph, basisphenoid; ch, choana; cqq, cranioquadrate groove; ec, ectopterygoid; exo-q s., exoccipital–quadrate suture; exo-sq s., exoccipital–squamosal suture; j, jugal; jf, jugal foramen; leu, lateral Eustachian opening; ltf, lower temporal fenestra; meu, median Eustachian opening; mx, maxilla; oc, occipital condyle; og, otic groove; or, orbit; po, postorbital; pt, pterygoid; q, quadrate; qj, quadratojugal; qjs, quadratojugal spine; sq, squamosal.

is represented as a prominent shelf on the anteromedial wall of the supratemporal fenestra of MMS/VBN-12-42 and makes the entire anterior wall of MMS/VBN-12-10A.

Postorbital: The postorbital contacts the frontal medially and the squamosal posteriorly and forms the

anterolateral corner of the supratemporal fenestra. In MMS/VBN-12-10A, the anterolateral postorbital corner has an anteroventral outgrowth overhanging a concavity, pierced by numerous foramina (Fig. 9C, D). The postorbital contributes to the postorbital bar and reaches along the internal side of the bar whereas the jugal makes most of the lateral surface of the bar. The

ventralmost process of the postorbital contacts the ascending process of the ectopterygoid (Fig. 9F). A slender posterior process contacts the quadratojugal at the dorsal corner of the infratemporal fenestra. The postorbital bar is cylindrical and more robust in the juveniles than in larger specimens. At midshaft level, there is a pronounced scar for muscle anchorage as seen in both skulls.

Squamosal: The squamosal is longer than the postorbital and forms the lateral and posterolateral edges of the supratemporal fenestra. The squamosal lateral margin overhangs the otic area; it is flat in MMS/VBN-12-10A, but has a small groove in MMS/VBN-12-42. Anteriorly, the lateral margin of the squamosal does not flare significantly. In dorsal view, the squamosal prongs of the small skulls MMS/VBN-12-42 and MMS/VBN-12-10D do not project significantly beyond the posterior margin of the skull table (Figs 2A, B, 7). This contrasts with the condition in MMS/VBN-12-10A (Fig. 3), where the squamosal prongs are pointed and project well beyond the posterior margin of the skull table. In the three specimens, however, the squamosal does not extend over the exoccipital.

Parietal: The parietal is preserved in MMS/VBN-12-10A, MMS/VBN-12-42 and MMS/VBN-12-10D. It makes the posteromedial and the medial margins of the supratemporal fenestrae. In dorsal view, the interfenestral width of the parietal is wider in the smaller individuals (MMS/VBN-12-42 and MMS/VBN-12-10D) than in the largest skull (MMS/VBN-12-10A). In the small specimens, the margin of the supratemporal fenestra is flat whereas a ridge is developed in the largest skull MMS/VBN-12-10A.

Supraoccipital: The supraoccipital is a reverse triangle in posterior view. It is robust and dorsoventrally expanded, but it does not seem to take part in the posterior edge of the skull table. Nevertheless, on the surface of the skull table of MMS/VBN-12-10A, there is a deep embayment that may correspond to the supraoccipital (Fig. 5A). Its occipital surface is marked by a robust median pillar. Dorsally in MMS/VBN-12-10A, two large protruding spines (the right one is broken off) are present at the medial corner of the posttemporal fenestrae. These protuberances are less developed in MMS/VBN-12-42.

Quadratojugal: The quadratojugal contributes to the entire posterior margin of the infratemporal fenestra and therefore makes its posteroventral corner. As it reaches the dorsal corner of the infratemporal fenestra, the quadratojugal excludes the quadrate posteriorly and the squamosal dorsally from the infratemporal fenestra (Fig. 9C, D). The dorsal tip of the quadratojugal con-

tacts a thin posterior process of the postorbital. The quadratojugal spine is robust, long and located in the middle sector of the posterior rim of the infratemporal fenestra in both the small MMS/VBN-12-42 and the large MMS/VBN-12-10A specimens (in the latter it is 8.1 mm long). In lateral view, the quadratojugal does not cover the lateral quadrate hemicondyle.

Quadrate: The lateral and medial quadrate hemicondyles of the juvenile specimens (MMS/VBN-12-10D and MMS/VBN-12-42) have roughly the same dimensions, contrasting with the situation in the largest specimen MMS/VBN-12-10A, in which the medial hemicondyle is small and ventrally reflected, whereas the lateral hemicondyle is twice as wide, but dorsoventrally thin (Fig. 5). The foramen aëreum is placed far from the medial edge and on the dorsal surface of the quadrate (Fig. 3). The foramen aëreum opens at the end of a modest ridge, at the level of the paroccipital process.

The otic region is well preserved in MMS/VBN-12-42, MMS/VBN-12-10D and MMS/VBN-12-10A. The siphonial foramen is circular and mostly opens through the quadrate, although its dorsal margin is formed by the exoccipital. Anterior to the siphonial foramen, the quadrate has a shallow depressed semicircular surface. This area is variably perforated: a preotic sinus is well developed in MMS/VBN-12-10D whereas foramina are absent in MMS/VBN-12-42, which has two large depressions instead: finally, MMS/VBN-12-10A lacks any perforation or depression in this area, with the exception of a minute foramen immediately ventral to the siphonial foramen (Fig. 8).

The ventral surface of the quadrate rami of the largest specimen MMS/VBN-12-10A shows a broad and weakly expressed elongated bump in the position of crest B of Iordansky (1973). At the level of the quadratojugal suture, just posterior to the infratemporal fenestra there is another moderate bump that may correspond to crest A of Iordansky (1973). Quadrate crests are more expressed in the smaller specimens. In MMS/VBN-12-42, the ventral surface of the left quadrate shows a crest close to the ventromedial border of the quadrate (crest B of Iordansky, 1973). Moreover, two small bumps close to the quadratojugal suture correspond to the area of crest A of Iordansky (1973). On the ventral surface of the quadrates of MMS/VBN-12-10D, there is a thin muscle scar that could correspond to scar A of Iordansky (1973) and a second broad and smooth structure that could correspond to scar B (Fig. 2).

Exoccipital: The exoccipital makes the posterior edge of the skull table and is visible in dorsal view in MMS/VBN-12-10A because of slight dorsoventral compression (Fig. 3). However, the rest of the skull table is not deformed in MMS/VBN-12-10A, suggesting that originally the exoccipital surface was not fully vertical, but

slightly sloping posteroventrally, a case observed in MMS/VBN-12-42, which does not show evidence of compression in the skull table area. The exoccipitals meet above the foramen magnum as a posteriorly projecting lamina, as observed in both MMS/VBN-12-10A and MMS/VBN-12-42. The ventral extent of the exoccipital is not visible around the foramen magnum. The opening for cranial nerve XII is visible in MMS/VBN-12-10A and in MMS/VBN-12-42, both at the level of the base of the foramen magnum. The foramen vagus (or cranial nerve X) is visible on the right side of MMS/VBN-12-42 only. It opens a short distance ventrolaterally to cranial nerve XII. In the same specimen, the foramen caroticus posterius is probably represented by a circular depression filled with sediment, placed at the ventrolateral edge of the exoccipital. The exoccipitals are laterally short. In MMS/VBN-12-42, the paroccipital processes host weakly expressed paroccipital bosses located close to the ventral edge of the bone. In MMS/VBN-12-10D, the paroccipital bosses, located close to the ventral tip of the exoccipital 'wings', are weakly expressed, being presented with a low, irregular rugosity. The paroccipital bosses are much more developed in the larger MMS/VBN-12-10A specimen where they are represented by a mediolaterally elongated ridge. Below this, the ventral surface of the paroccipital process consists of a robust lamina that projects over the quadrate medial branch.

Cranioquadrate groove: All four skulls have a congruent morphology of the cranioquadrate groove (Fig. 9A, B). The dorsal surface of the quadrate hosts the otic groove, which consists of a smooth channel connected anteriorly to the syphonia foramen and is laterally bordered by a marked crest of the quadrate (this crest ends curving laterally at the level of the posterior tip of the paroccipital process). Medial to the otic groove is a step-like structure corresponding to the quadrate–exoccipital suture that extends from the level of the syphonia foramen to the posterior edge of the skull. Above the suture, the exoccipital is deeply excavated as a laterally opened cranioquadrate groove – clearly visible in lateral view – roofed by the squamosal. The cranioquadrate passage is open in all skulls, but it is proportionally narrower in MMS/VBN-12-42 and MMS/VBN-12-10D than in MMS/VBN-12-10A. It is not clear if this reflects an ontogenetic difference or if, more probably, it results from deformation that pushed upwards the quadrate surface of the small specimens. In posterior view (Fig. 6), the exit area of the cranioquadrate canal is a large ovoid concavity of the quadrate bordered laterally by the dorsal quadrate crest and dorsally by the exoccipital lamina.

Basioccipital, basisphenoid and laterosphenoid: The basioccipital plate is fully vertical and is wider than

high. Its ventral margin is excavated medially, where the median Eustachian foramen opens. There is a median vertical keel separating both areas of the plate, which is more robust in the large specimen. The occipital condyle and foramen magnum are wider than high. The basisphenoid is partly visible in MMS/VBN-12-10A, where it is restricted to a thin lamina between the posteromedial process of the pterygoid and the basioccipital (Fig. 9G). Here, the large circular median Eustachian foramen opens posteroventrally. The basisphenoid does not project ventrally along the surface of the pterygoid. The lateral Eustachian foramina are barely discernible and are smaller than the median Eustachian foramen. The laterosphenoid is visible only on the right side of MMS/VBN-12-10D. It preserves its anterior suture, which is clearly not transversally orientated, but oblique as in all derived eusuchians.

Pterygoid: The pterygoids are complete in MMS/VBN-12-10A and partly preserved in MMS/VBN-12-42, near the suborbital fenestra. In MMS/VBN-12-10A, the pterygoid surface is moderately convex in the area anterolateral to the choana. The posteromedial pterygoid processes are tall and quite prominent, with a marked U-shaped profile in ventral view. Lateral to these processes, the posterior margin of the pterygoid wing is notched and the posterolateral corners of the wings taper further posteriorly than the posteromedial processes. The lateral surface of the pterygoid torus transiliens is flat and densely vascularized. The internal choanae open on the posterior half of the pterygoids, close to the posterior margin of the palate (Fig. 3).

Ectopterygoid: The ectopterygoid builds the medial wall of maxillary alveoli 12 and 13 and forms the posterolateral border of the suborbital fenestra where it has a concave outline near its anterior tip. The anterior pointed process of the ectopterygoid reaches the level of alveolus 11. In MMS/VBN-12-10A, the ectopterygoid–pterygoid suture preserves the flexure. The ectopterygoid does not reach the tip of the pterygoid wing, as seen in MMS/VBN-12-42 and MMS/VBN-12-10A (Figs 2, 4).

Palatine: In MMS/VBN-12-42 the anterior palatine process is blunt, subrectangular and ends at the level of the 6th alveolus (Fig. 4D). In MMS/VBN-12-10A, the anterior edge of this process could correspond to a breakage, as tentatively shown in Figure 4B. The anterior rim of the suborbital fenestra stops at the anteriormost margin of the 7th alveolus. The palatine–pterygoid suture is close to the posterior corner of the suborbital fenestrae, but it is nevertheless located on the interfenestral bar. A longitudinal groove extends

medially along the palatines, at their contact between the suborbital fenestrae.

Dentary: MMS/VBN-12-10B consists of a right dentary (Fig. 10) found in close association with the skull MMS/

VBN-12-10A. The region from the anterior rim of the fourth alveolus to the sutural scar left by the surangular is preserved. There are a total of 13 alveoli preserved in this specimen, with the largest possibly corresponding to the 4th. Therefore, this dentary might

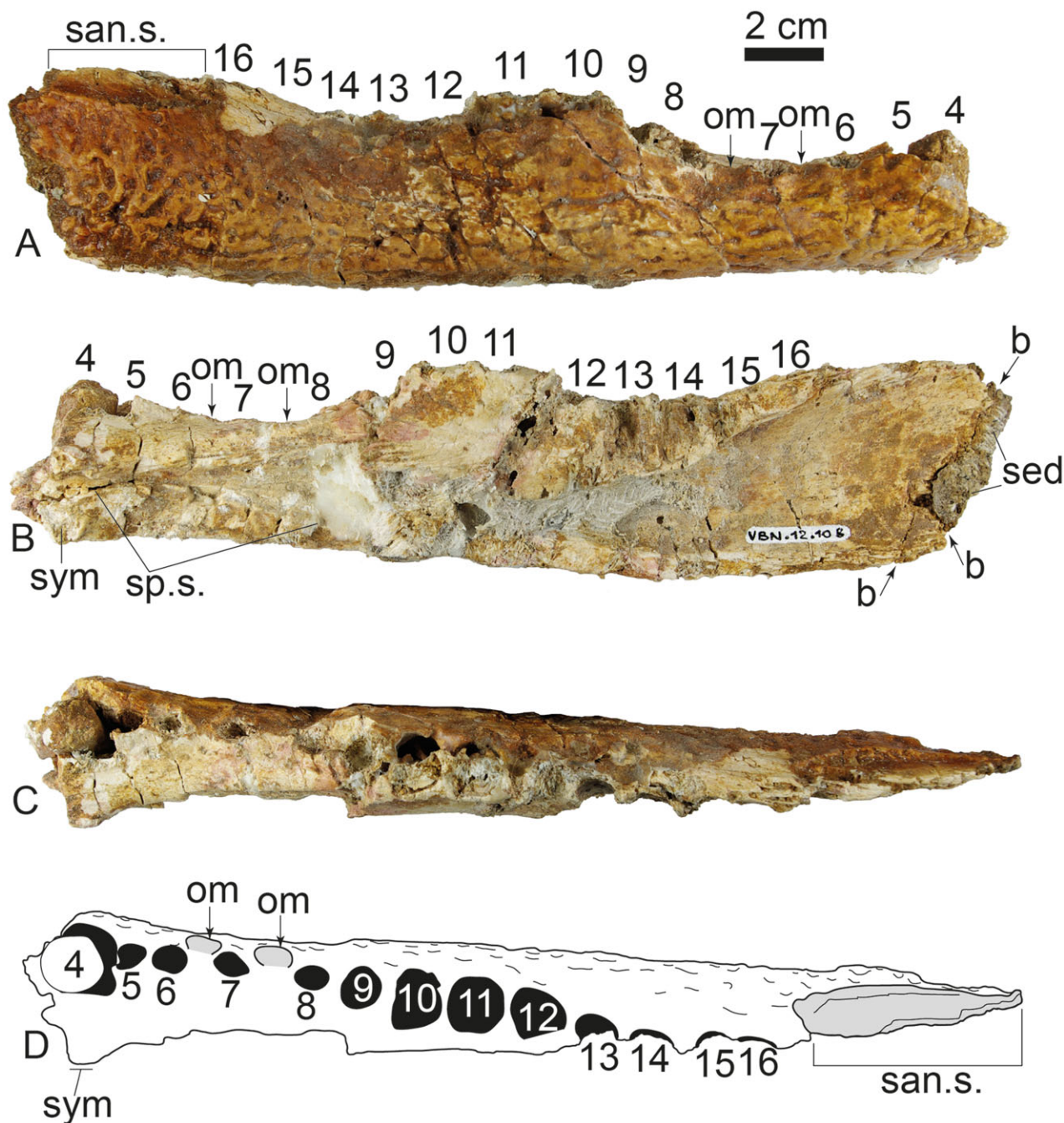


Figure 10. The anterior portion of the right mandibular ramus of *Allodaposuchus precedens* Nopcsa, 1928 (MMS/VBN-12-10B) from the Campanian of Velaux-La Bastide Neuve, France in A, lateral, B, medial and C, occlusal views; D, interpretative drawing in occlusal view. Abbreviations: b, break; om, occlusal mark; san.s., surangular suture of the dentary; sed, sediment; sym, symphysis; sp.s., splenial suture of the dentary. Numbers denote tooth positions with 4 indicating the anteriormost preserved alveolus.

have hosted a total of 16 alveoli. In lateral view, the dentary has two pronounced waves. First, a marked concavity extends between the fourth alveolus and the tenth alveolus. Here, the 10th interalveolar space corresponds to the apex of the convexity. More posteriorly, the tooth row is slightly concave until the last alveolus. There is a short diastema between the 6th and 7th alveoli, then a larger one between the 7th and 8th alveoli. At the level of these diastemae, there are occlusal marks on the lateral surface of the dentary for reception of the maxillary dentition. Ornamentation is dense on the lateral surface of the dentary and consists of marked furrows separated by bony overgrowths. Near the posterior margin of the dentary, at the level of the surangular suture, the ornamentation is weaker or absent and the dentary becomes thinner. Given the position of the surangular suture on the dentary, an external mandibular fenestra is considered absent (Fig. 10). In its anterior region, the dentary forms a flat and large ventral surface. The symphysis starts at the level of the fourth alveolus. In medial view, the suture for the splenial seems to end posterior to the symphysis, not taking part in it. The anteriormost process of the surangular ends just posterior to the last alveolus.

OCCLUSION PATTERN

Premaxilla: Both MMS/VBN-12-10A and MMS/VBN-12-42 preserve a notch at the level of the premaxillary–maxillary suture, which receives the largest dentary tooth.

Maxilla: In MMS/VBN-12-10A, the arrangement of the first three alveoli is anomalous on both right and left rows. Here, these alveoli have a triangular arrangement (Fig. 4). This contrasts with the arrangement seen in the smaller specimen MMS/VBN-12-42. In MMS/VBN-12-42, both the right and the left maxillary tooth rows show a pit between the sixth and seventh alveoli. This pit is shallow (6.7 mm wide by 4.6 mm long), but its rims are well delineated between alveoli. In the left maxilla MMS/VBN-93-29, occlusal pits are clearly visible at the level of the 6th (inline), 7th and 8th (medially placed) interalveolar spaces, signifying a change in the occlusion from fully inline to a clear overbite. In the right maxilla MMS/VBN-93-30, the pits are equally developed and placed, but this specimen hosts a further pit placed medially to the small ninth interalveolar space. In the largest specimen MMS/VBN-12-10A, there are possible occlusal pits medial to the interalveolar spaces from 6 to 8 on the right side and from 5 to 8 on the left side there.

Dentary: The tooth row of MMS/VBN-12-10B mirrors the right tooth row of the skull VBN-12-10A and

matches the size of the maxillary tooth row. The largest fourth dentary alveolus fits in the premaxillary–maxillary notch and the largest lateral depression near the eighth dentary alveolus matches the largest fourth maxillary alveolus. The tenth large dentary alveolus also matches the concavity at the level of the sixth and seventh maxillary alveoli, where a set of four medially placed occlusal pits are visible on the maxilla. The last dentary tooth corresponds to the eleventh maxillary alveolus. There is a notch resulting from the occluding maxillary dentition on the lateral surface of the dentary between the seventh and eighth alveoli, which is 20.2 mm in height, then another notch between the eleventh and twelfth alveoli and finally one just below the thirteenth alveolus.

Dentition: In MMS/VBN-12-10A, teeth are preserved in alveoli 5 and 9 on the right maxilla and alveoli 3 and 4 on the left. Teeth are conical with two well-developed mesiodistal carinae delimiting a wide labial from a narrow lingual surface. Each carina is smooth and well marked and both sides of the tooth bear vertical ridges (Fig. 11). They are identical to one of the teeth in the *Allodaposuchus precedens* skull from Romania (Delfino *et al.*, 2008a), in the *Allodaposuchus* cf. *precedens* skull from Var (Martin, 2010), in *Allodaposuchus subjuniperus* (Puértolas-Pascual *et al.*, 2013) and in *Allodaposuchus palustris* (Blanco *et al.*, 2014). In addition, this morphology is observed in the teeth associated with the holotype of *Ischyrochampsia meridionalis* (Fig. 11). Although we did not examine the specimens of *Musturzabalsuchus* first-hand, it is noteworthy to add that the figured specimen MCNA 7480 has teeth with a similar morphology and that the lateral view available in Csiki-Sava *et al.* (2015) shows evident vertical ridges on the labial surface of the teeth.

POSTCRANIUM

Femur: MMS/VBN-02-37 consists of a complete left femur (Fig. 12). It is stout and markedly sigmoid with an expanded and dorsoventrally flattened proximal head. The fourth trochanter is remarkably large and faces fully ventrally instead of being located on the lateral edge. Mediodorsal to this trochanter, there is a deep slit-like depression. Distally, the condyles are not aligned, the lateral one being thick, wide and tapering further anteriorly than the medial one. A deep excavated trochlea separates both condyles on the dorsal surface and extends proximally for 6 cm.

Osteoderm: One osteoderm (MMS/VBN-12-10F, Fig. 12) has been recovered in the vicinity of the large skull. It is 8 cm long and 5.6 cm wide. There is a hint of a

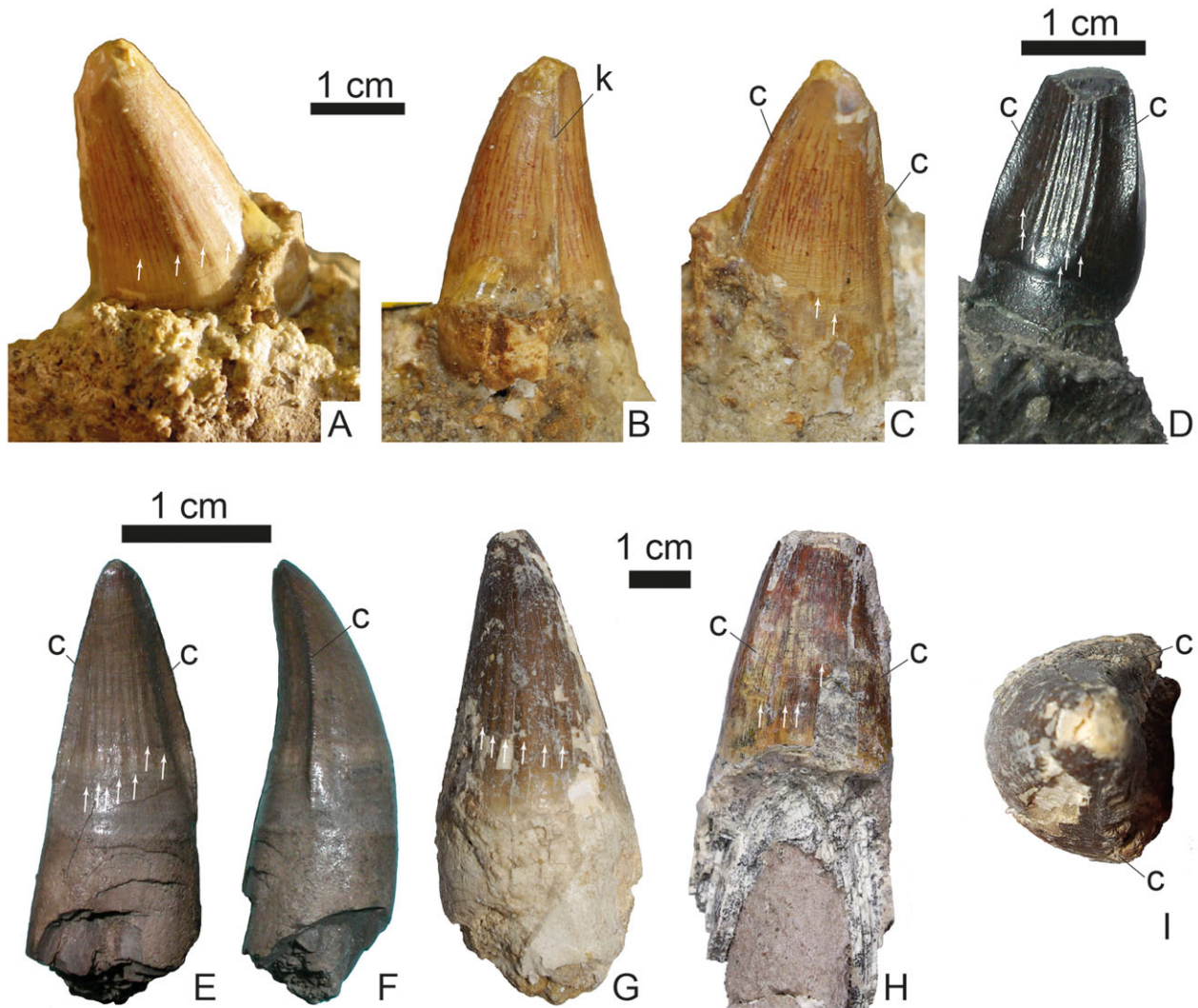


Figure 11. Details of the morphology of the fourth left maxillary tooth of *Allodaposuchus precedens* Nopcsa, 1928 (MMS/VBN-12-10A) in A, labial, B, mesial and C, lingual views. D, first right maxillary tooth of *A. precedens* from Oarda de Jos (PSMUBB V 438) in lingual view; isolated tooth crown (MFGI 12685) attributed to *A. precedens* in E, lingual and F, mesial or distal views; the dentition of *Ischyrochampsia meridionalis* (MNHN) in G, labial, H, lingual and I, apical views. White arrows indicate vertical ridges on the labial and lingual surfaces of crowns; c, mesiodistal carina.

median ridge extending along its dorsal surface, which ends posteriorly at the level of the maximum convexity of the posterior margin. The osteoderm has nearly parallel edges marked by thick sutural areas along their entire margins. It is thick and covered by numerous deep ovoid anastomosing pits, except in the anterior area, which is thin and forms a smooth surface less than 2 cm long and corresponds to the anterior articular facet. The right corner of this articular facet is broken off, but the left side is complete and seems to taper further anteriorly. The ventral surface is completely smooth.

DISCUSSION

AFFINITIES OF *ALLODAPOSUCHUS PRECEDENS*

The three nearly complete skulls (MMS/VBN-12-10A, MMS/VBN-12-42 and MMS/VBN-93-28) share diagnostic features for *Allodaposuchus precedens* such as the laterally open cranioquadrate groove, participation of the nasal into the external nares, ectopterygoid adjacent to the posterior margin of the maxillary tooth row, very large fourth maxillary alveolus and a maxillary alveolar count of 13. Although one specimen is fragmentary and represented only by a skull table

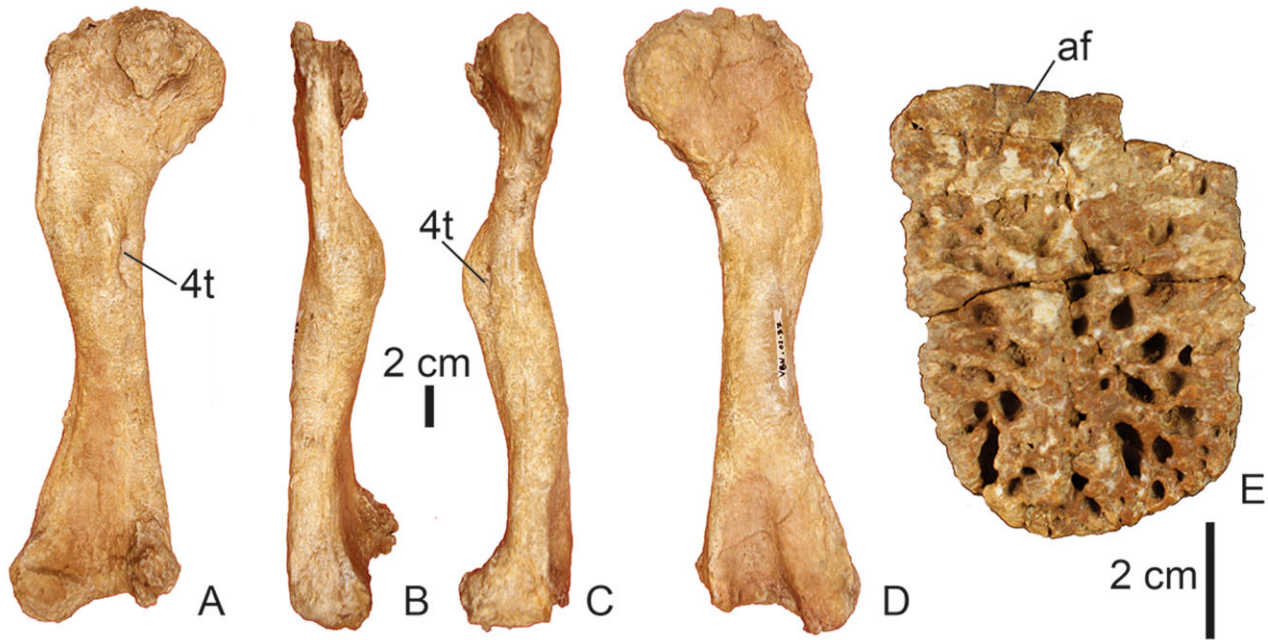


Figure 12. Postcranial elements associated with *Allodaposuchus precedens* Nopcsa, 1928. Cast of the left femur (MMS/VBN-02-37) in A, ventral; B, lateral; C, medial; and D, dorsal views. E, isolated osteoderm (MMS/VBN-12-10F) in dorsal view. Abbreviations: 4t, fourth trochanter; af, anterior facet.

(MMS/VBN-12-10D), it is similar in size to MMS/VBN-12-42, which shares the open cranioquadrate groove, a similar ornamentation pattern and overall skull proportions. There is therefore no doubt that all specimens belong to a single taxon and represent various growth stages. The results of the phylogenetic analysis of *Allodaposuchus precedens* based on the MMS/VBN specimens are congruent with the results recovered by Brochu *et al.* (2012). For this reason and for ease of reading, the consensus tree is simplified with several taxa having derived positions in the crown group collapsed into major clades (Fig. 13) (54 trees retained; best tree length = 655; consistency index = 0.346; retention index = 0.815). Minor alterations concern the base of Eusuchia with a well-resolved hypothesis involving *Iharkutosuchus makadii* + *Hylaeochampsia vectiana* as the most derived hylaeochampsid clade. *Acynodon adriaticus* and *Acynodon iberoccitanus* occupy a basal position in this group and *Allodaposuchus precedens* occupies the basalmost position in the monophyletic hylaeochampsid clade.

ONTOGENY

The range of skull lengths (from the anterior tip of the premaxilla to the posterior edge of the supraoccipital) measured in the complete skulls from VBN are between 173 and 411 mm (see Supporting Information Appendix S1 and Fig. 15). Including specimens described in

the literature, the current sample size of relatively complete *Allodaposuchus* skulls includes six individuals, in addition to the three VBN skulls. This includes material assigned to *A. precedens* from Romania (Delfino *et al.*, 2008a), *A. cf. precedens* from France (Martin, 2010) and *A. subjuniperus* from Spain (Puértolas-Pascual *et al.*, 2013). Moreover, a complete skull was illustrated in the field at the site of Lo Hueco, Spain, and briefly referred as *Musturzabalsuchus* (Ortega *et al.*, 2008) and could represent an additional specimen of *Allodaposuchus* (Narváez *et al.*, 2013; Csiki-Sava *et al.*, 2015).

Plotting skull width vs. skull length reveals that the skull of *Allodaposuchus* was growing isometrically (the slope of the regression line is very close to 1, Fig. 15), as is also the case in *Acynodon*. However, there are only three complete skulls of *Acynodon* and they are all of similar, small sizes, so whether isometric growth is a shared characteristic of *Acynodon* and *Allodaposuchus* has yet to be demonstrated with more complete skulls representing an ontogenetic series in *Acynodon*. As a comparison, skulls of extant taxa represented by a short-snouted crocodyline *Osteolaemus tetraspis* and a mesorostrine crocodyline *Crocodylus niloticus* were plotted with *Allodaposuchus* and *Acynodon*. Both *Osteolaemus tetraspis* and *Crocodylus niloticus* measurements fall on a regression line with a slope of ~0.7, indicating that larger specimens have a narrower skull than smaller ones.

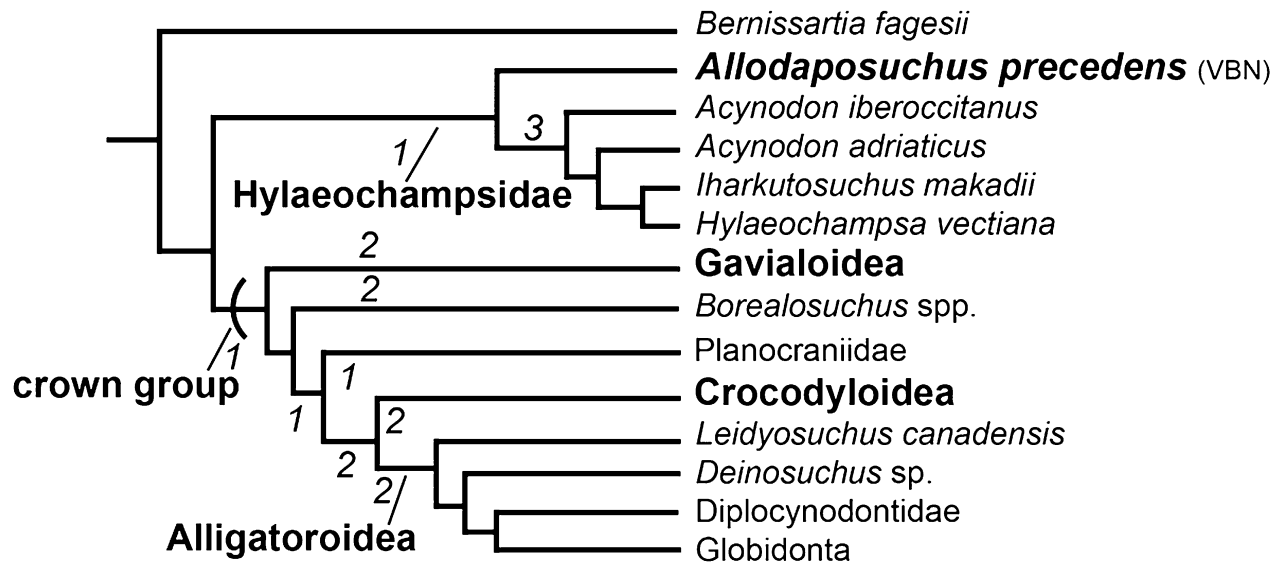


Figure 13. Phylogenetic results of the inclusion of the VBN skulls of *Allodaposuchus precedens* in the matrix of Brochu *et al.* (2012). Numbers represent Bremer decay indices.

The VBN specimens permit tracing of the following morphological changes in the course of *Allodaposuchus* ontogeny (compare Figs 2–6, 8). The general outline of the skull is affected by the accentuation of some features such as the widening profile of the rostrum in dorsal view at the level of the largest alveolus; the development of a depression on the dorsal surface of the jugal; the lateral contour of the nasal near its anterior margin, which changes from gently shrinking to shrinking with an acute angle in the adult; widening of the quadrate and quadratojugal; the bulging contour of the orbits and supratemporal fenestrae, accompanied by a modification of the dorsal surface of the frontal and parietal from flat to excavated; narrowing of the space between the supratemporal fenestra accompanied by a slight lateral expansion of the fenestrae; the relative size of the orbits becoming smaller; and the development of the squamosal prongs that project posteriorly in the adult. Muscle scars on the ventral surface of the quadrate are thin in the juvenile specimens and become broader and shallower in adults. Paroccipital bosses are barely developed in the juveniles, but become a massive point of muscle attachment in adults. The incisive foramen is large in juveniles, but is reduced to a small opening in adults. The external nares shift in position and become larger and anteroposteriorly elongated in the adult. The quadrate hemicondyles are not significantly different in shape in the juvenile, but in the adult, the medial hemicondyle is ventrally reflected, implying a change in the articulation and constraints transmitted through the mandible. It is uncertain whether the adult skull VBN-12-10A possesses fewer premaxillary alveoli than the

juvenile skull VBN-12-42. Finally, the postorbital bar is robust in the juvenile (MMS/VBN-12-42) and is slender in the adult (MMS/VBN-12-10A). Because of their variability, those characters must be regarded with caution when erecting new species of *Allodaposuchus* or for the purposes of phylogenetic investigations.

By contrast, the following characters do not change in the course of ontogeny: the presence of a premaxillary–maxillary notch both in the juvenile and in the adult form; the number of maxillary alveoli (13); the maxillary tooth row (from alveoli 1 to 7) is in a ventral position relative to the palatal surface of the maxilla; the frontoparietal suture penetrates between the supratemporal fenestrae; the quadratojugal spine remains acute and robust; the cranioquadrate groove opens laterally into the skull table; the foramen aëreum opens on the dorsal surface of the quadrate; the ectopterygoid does not reach the posterior tip of the pterygoid wing and the anterior process of the ectopterygoid borders the last two alveoli. The variable and stable characters during ontogenetic change in the VBN *Allodaposuchus* skulls provide a new perspective to test the recently augmented taxonomic content of *Allodaposuchus*.

HOW MANY SPECIES OF ALLODAPOSUCHUS?

Until recently, only one species of *Allodaposuchus*, *A. precedens* Nopcsa, 1928, was recognized (Buscalioni *et al.*, 2001; Delfino *et al.*, 2008a). The attribution of a skull to *Allodaposuchus* cf. *precedens* from southern France (Martin, 2010) opened the possibility that this specimen might represent a new species (Puértolas-Pascual

et al., 2013) different from both *Allodaposuchus precedens* and from the recently erected new species, *Allodaposuchus subjuniiperus* and *Allodaposuchus palustris* both from the Maastrichtian of Spain (Puértolas-Pascual *et al.*, 2013; Blanco *et al.*, 2014). All these taxa were erected on the basis of single individuals that do not provide information about ontogeny or variability, as frequently happens in fossil crocodylians (Delfino & Sánchez-Villagra, 2010). The discovery of several specimens in the VBN locality provides a basis for appreciating the morphological variability encountered in the *Allodaposuchus* hypodigm (see previous discussion) and allows us to test whether the French population is distinct or not from *Allodaposuchus precedens* from Romania and from *A. subjuniiperus* and *A. palustris* from Spain.

We do not find evidence for distinguishing specimens of *Allodaposuchus* from France (Var, Martin, 2010; or from VBN) and Romania (see Delfino *et al.*, 2008a). The preorbital ridge described in *Allodaposuchus* cf. *precedens* from France (Martin, 2010) has never been observed in *A. precedens* from Romania (Delfino *et al.*, 2008a). The preorbital ridge in *A. cf. precedens* could be considered as an artefact of preservation involving the compression of bones making the orbital contour, which is bulged. This is supported by the deformed nature of the *A. cf. precedens* skull described by Martin (2010) and by the absence of such a preorbital ridge in the undistorted VBN skulls. A pair of depressions has been reported on the surface of the maxilla of *A. cf. precedens* (Martin, 2010). As initially proposed, it is possible that this results from deformation/collapse of the skull. This is also supported by the fact that such depressions have not been observed in any other specimens of *Allodaposuchus* from France. The specimens from VBN, but also the specimen from Var described by Martin (2010), share the same combination of characters as the specimens of *Allodaposuchus* from Romania (Delfino *et al.*, 2008a), and for this reason we consider that the French and Romanian specimens belong to *A. precedens*.

According to Puértolas-Pascual *et al.* (2013), *Allodaposuchus subjuniiperus* differs from all other specimens referred to *Allodaposuchus* by its incisive foramen located close to the premaxillary–maxillary suture, the presence of four premaxillary alveoli, the outline of the nasals, relatively small orbits and a remarkably wide frontal, wider than the orbital diameter. We recognize that in general outline, the skull of *A. subjuniiperus* is dissimilar to *A. precedens* from Romania and France, notably regarding the relative size of the orbits and the width of the frontal bone. Moreover, the rostrum of *A. subjuniiperus* appears longer than any rostrum described for *Allodaposuchus*. Admittedly, all members of the genus *Allodaposuchus* are characterized by a nasal that considerably diminishes in width in its ante-

rior region; however taking the outline of the nasal as a diagnostic character at the species level is questionable considering variation observed in all the VBN skulls and *A. precedens* from Romania (see previous discussion). In *A. subjuniiperus*, the morphology of the premaxilla is remarkably short along the anteroposterior axis and the premaxilla possesses four alveoli, vs. five in all other *Allodaposuchus* specimens (although in MMS/VBN-12-10A this count is uncertain). Therefore, could the position of the incisive foramen and the low number of premaxillary alveoli be the result of a pathology? As exemplified by the MMS/VBN-12-10A specimen, morphological oddities may be common. The largest skull of *Allodaposuchus* (MMS/VBN-12-10A) presents an anomalous arrangement of the first three maxillary alveoli, on both maxillae. These alveoli are not aligned but are organized in a triangular pattern. The skull MMS/VBN-12-10A did not experience deformation in this area and we consider these alveoli as pathological, resulting from the growth of teeth in a limited space. Whether some of the diagnostic traits of *A. subjuniiperus* (position of incisive foramen, number of premaxillary alveoli) are pathological or are the expression of ontogenetic variability might only be tested by recovering more specimens.

Blanco *et al.* (2014) recently described a new species of *Allodaposuchus*, *A. palustris*, on the basis of fragmentary cranial and postcranial remains from the Late Cretaceous of Fumanya, Spain. *Allodaposuchus palustris* is diagnosed on the basis of the absence of shallow fossa on the rostromedial margin of the supratemporal fossa; a slightly concavoconvex frontoparietal suture; an exoccipital without a boss on the paroccipital process; a large foramen aëreum; short, robust teeth with marked longitudinal grooves close to carinae; false-zipodont crenulations; and anterior process of ilium more developed. The development of the anteromedial margin of the supratemporal fossa is impossible to assess in the material referred to *A. palustris* because it is incomplete; the morphology of the frontoparietal suture is comparable to the condition in the VBN skulls and in other *Allodaposuchus* specimens (Buscalioni *et al.*, 2001; Delfino *et al.*, 2008a; Martin, 2010; Puértolas-Pascual *et al.*, 2013); the expression of the boss on the paroccipital process falls within the observed ontogenetic variability described in this work for the VBN skulls; and the size of the foramen aëreum is non-diagnostic, as the dorsal wall of the duct can be easily broken off. Moreover, the foramen aëreum is known to vary in shape even within a single species, sometimes being characterized by multiple openings (see *Diplocynodon* in Martin *et al.*, 2014b). The ‘very marked longitudinal grooves close to the carinae’ of *A. palustris* (Blanco *et al.*, 2014: 9) are clearly present in the type material of *A. precedens* (Fig. 11) and were actually described by Buscalioni *et al.* (2001) for the

A. precedens material from Armuña, Spain, and by Delfino *et al.* (2008a) for the *A. precedens* material from Vălioara, Romania. Regarding the degree of false-zipodont crenulations expressed by the carinae of the teeth of *A. palustris*, we note that the isolated teeth associated with the type material of *A. precedens* (Fig. 11) do also possess false-zipodont crenulations (*sensu* Prasad & de Lapparent de Broin, 2002). This was explicitly described as delicately wrinkled in the material from Armuña (Buscalioni *et al.*, 2001, see hatches close to the carinae in their fig. 14). For this reason, the carinae of *A. precedens* from Vălioara were also described as smooth (Delfino *et al.*, 2008a), but at least some of the few available teeth show the same morphology described above (Fig. 11). The morphology of the ilium is only partly known in the type material of *A. precedens*, but this bone was not found associated with other skull materials of *A. precedens* (Buscalioni *et al.*, 2001) or *A. subjuniperus*. Due to the lack of diagnostic characters at the species level for *A. palustris*, we propose to refer the material described by Blanco *et al.* (2014) to *Allodaposuchus* sp.

In conclusion, *Allodaposuchus* can be safely recognized on the basis of *A. precedens* from France and Romania. The taxonomic status of *A. subjuniperus* from Spain needs confirmation and the recently erected *A. palustris* from Spain lacks sufficient diagnostic characters to be retained. The numerous remains of *Allodaposuchus* recently recovered from Lo Hueco (Ortega *et al.*, 2008; Narváez *et al.*, 2013) will certainly provide a solid basis for further testing the taxonomic content of the genus *Allodaposuchus* in the Late Cretaceous of the Iberian Peninsula.

THE TAXONOMIC STATUS OF *MUSTURZABALSUCHUS* AND *ISCHYROCHAMPSA*

Description of the VBN specimens allows us for the first time to confidently assign a dentary bone (MMS/VBN-12-10B found in association with the skull MMS/VBN-12-10A) to the genus *Allodaposuchus*. Whether *Allodaposuchus precedens* and *Musturzabalsuchus buffetauti* (Buscalioni *et al.*, 1997, 1999) represent the same taxon has already been questioned (Martin, 2010). The specimen MMS/VBN-12-10B (Fig. 10) and *M. buffetauti* share the following features of the dentary: an enlarged fourth dentary alveolus located at the level of the posterior end of the symphysis; a diastema between the seventh and eighth alveoli; an occlusion mark lateral to this diastema; the ventral surface of the dentary being broad and flat in the symphyseal area; the dorsal edge of the dentary being festooned in lateral view; at the level of the surangular suture, the ornamentation of the dentary is weaker or absent and the dentary becomes thin; the extension of the splenial that stops at the posterior end of the dentary symphysis;

the fifth dentary alveolus extremely reduced relative to the fourth; and the likely absence of an external mandibular fenestra. In addition, both taxa may share 16 dentary alveoli. Although the posterior region of the dentary MMS/VBN-12-10B is broken off, the observed number of 16 alveoli could be close to the complete count because of the presence of the surangular suture that indicates the end of the tooth row. Finally, the dentition of *M. buffetauti* described with sharp carinae, and the crown surface profusely ridged with the margin crenulated (Buscalioni *et al.*, 1999: 219) is reminiscent of the morphology in *Allodaposuchus* (Buscalioni *et al.*, 2001; Delfino *et al.*, 2008a; Martin, 2010; Blanco *et al.*, 2014; see also Fig. 11). Although we have not seen *M. buffetauti* first-hand, these similarities are striking and invite the evaluation of the synonymy of *M. buffetauti* with *Allodaposuchus* when more complete mandibular specimens become available.

The trematochampsid *Ischyrochampsia meridionalis* was erected on the basis of the extremity of a rostrum and relatively complete, albeit poorly preserved mandibular rami from the Late Cretaceous of Saint-Estève Janson, Bouches-du-Rhône, France (Vasse, 1995). In his diagnosis of *I. meridionalis*, Vasse (1995) noted the following characters that now show striking resemblances with *Musturzabalsuchus* (Buscalioni *et al.*, 1997, 1999): short mandibular symphysis extending back to the level of the fourth alveolus; splenial that reaches but does not participate in the symphysis; the first, fourth and eleventh alveoli are the largest; and robust teeth with 'mousse' apex, smooth carinae and crown surface with ridges. As in *A. precedens*, the teeth of *I. meridionalis* (Fig. 11G, H) are conical, recurved and possess sharp mesiodistal carinae, which are shifted on the lingual side of the crown. Ridges ornament the crown surface on both the lingual and the labial sides. Vasse (1995) reported a total of 11 dentary alveoli. However, the condition of preservation of the specimen referred to *I. meridionalis* obscures the last alveoli and it is probable that this specimen hosts at least 15 alveoli (Fig. 14). Vasse (1995) also identified an external mandibular fenestra, but direct examination of the specimen reveals that it corresponds to a break, indicating that an external fenestra is probably absent, as in the mandible of *M. buffetauti*. Recent re-examination of *I. meridionalis* reveals that no diagnostic characters could be validated for this taxon. The mandible of *I. meridionalis* has experienced considerable crushing as evidenced from several fractures, as already noted by Vasse (1995). In lateral view, the posterior mandibular ramus is collapsed and possibly some anatomical features have been slightly displaced. As such, a large mark of occlusion is present on the lateral side of the dentary of *I. meridionalis* at the level of the eighth or maybe the ninth alveolus (Fig. 14). In

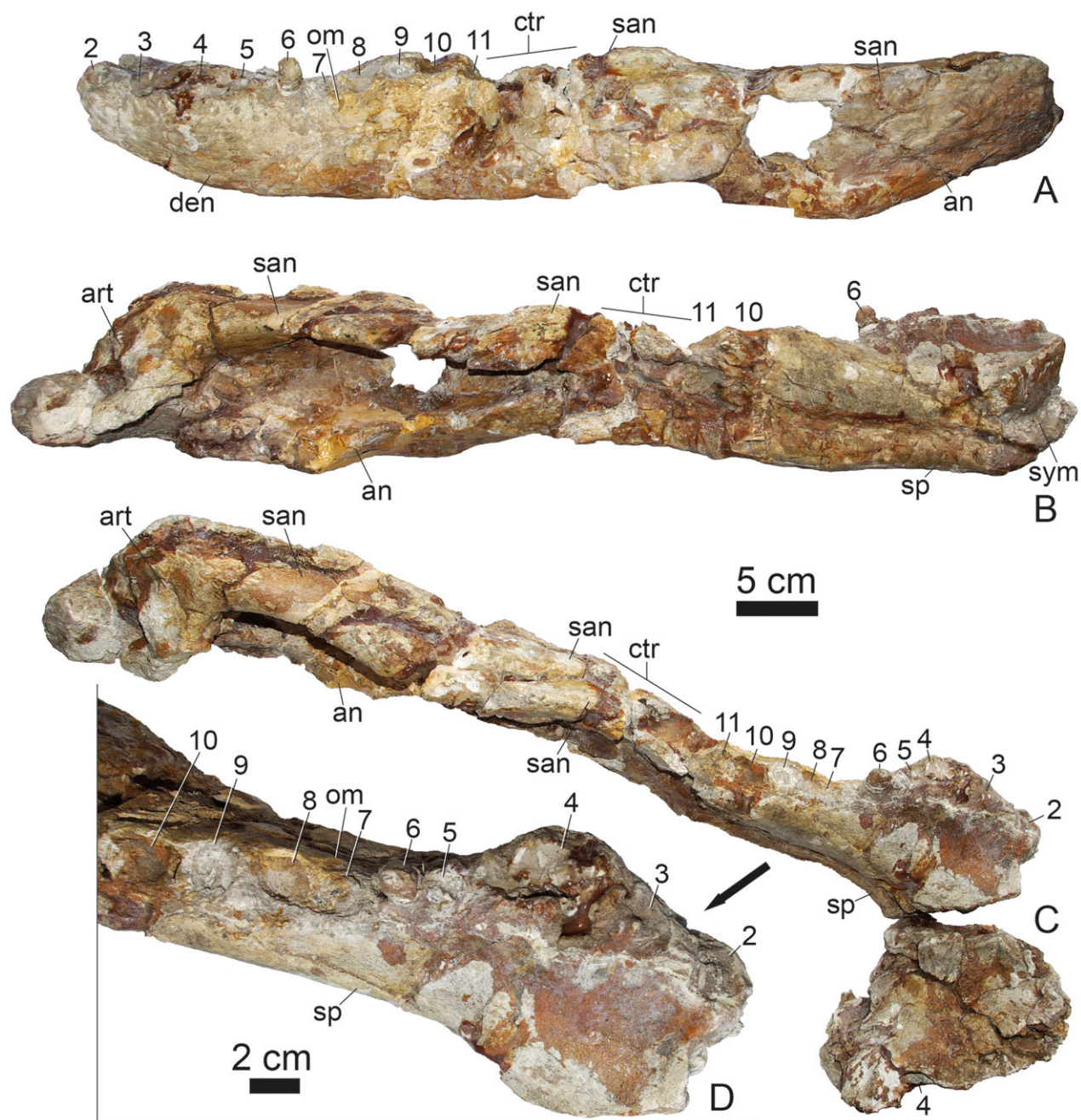


Figure 14. The mandible of *Ischyrochampsia meridionalis* Vasse, 1995, presently identified as *Allodaposuchus* sp. Left ramus in A, lateral and B, medial views; both rami in C, occlusal view; detail of the anterior portion of the left ramus in D, occlusal view. Abbreviations: an, angular; art, articular; ctr, crushed tooth row; om, occlusal mark; san, surangular; sp, splenial; sym, symphysis. Numbers denote tooth positions with 2 indicating the anteriormost preserved alveolus.

MMS/VBN-12-10B and in *M. buffetauti*, this occlusion mark is placed between the seventh and the eighth alveoli. Other features cannot be checked on MMS/VBN-12-10B, but are readily comparable in the mandibles of *M. buffetauti* and in *I. meridionalis*. In these, the surangular has a mediolaterally developed dorsal

surface; the tooth row is slightly shorter than the posterior region of the edentulous mandibular ramus.

Comparison of the mandible MMS/VBN-12-10B with two other taxa from the Late Cretaceous of Europe, *Musturzabalsuchus* and *Ischyrochampsia*, leads to the conclusion that the latter two taxa could reasonably

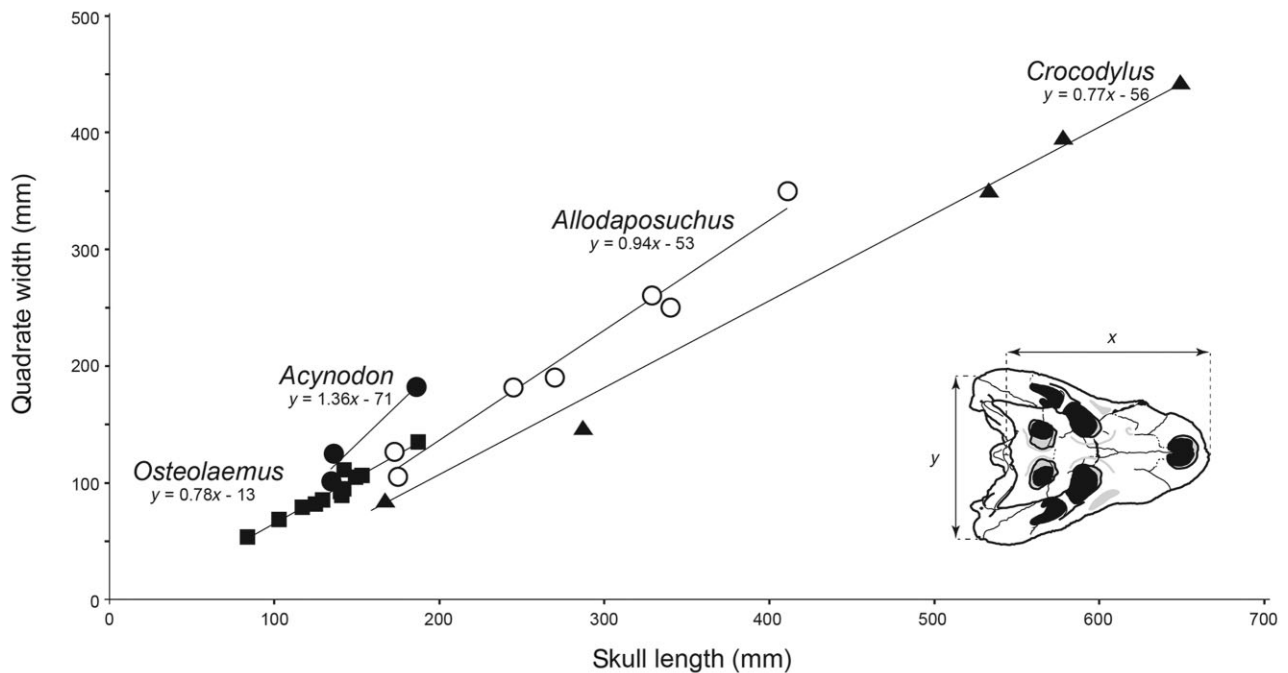


Figure 15. Cranial measurements in selected eusuchians plotting quadrate width vs. skull length (in mm). Open circles: *Allodaposuchus precedens* ($N = 7$); filled circles: *Acynodon* ($N = 3$); filled triangles: *Crocodylus* sp. ($N = 5$); filled circles: *Osteolaemus tetraspis* ($N = 13$). Measurements and sources of the specimens are given in Supporting Information Appendix S1.

represent junior synonyms of *Allodaposuchus*. Alternatively, because of the absence of clearly diagnostic characters, *Ischyrochampsia meridionalis* should be considered a *nomen vanum* (*sensu* Sanchíz, 1998). Of note is that *I. meridionalis* was originally considered as a non-eusuchian taxon with Gondwanian affinities (Vasse, 1995), but this hypothesis is no longer supported and the diversity of non-eusuchians in the Late Cretaceous of Europe is restricted to the genera *Theriosuchus* and *Doratodon* (Martin & Delfino, 2010; Martin, Rabi & Csiki, 2010; Martin *et al.*, 2014a; Rabi & Sebök, 2014).

HYLAEOCHAMPSIDS AS EUROPEAN ENDEMICS

During the Late Cretaceous, Europe was an archipelago, and this palaeogeography seems to have favoured local endemism in some tetrapod groups (Csiki-Sava & Grigorescu, 1998; Grigorescu *et al.*, 1999; Weishampel *et al.*, 2010; Csiki-Sava *et al.*, 2015). However, the relative small size of Europe and the swimming capacities of eusuchians make it unlikely that there were multiple localized areas of endemism for different species of *Allodaposuchus* in Europe. As a comparison, today's distribution of species of *Crocodylus* rarely overlaps, and when this is the case, different species have different body size (compare *Crocodylus porosus* with *Crocodylus johnstoni*; Webb,

Manolis & Sack, 1983). Indeed, it cannot be excluded that different species of *Allodaposuchus* occurred through time, as was suggested for the most recent species *Allodaposuchus subjuniiperus* (Puértolas-Pascual *et al.*, 2013) and *Allodaposuchus palustris* (Blanco *et al.*, 2014), but this will have to be confirmed with more than one specimen. On the other hand, we demonstrate here that *Allodaposuchus* from southern France does not form a separate species as was recently proposed (Puértolas-Pascual *et al.*, 2013), but can be unequivocally allied to *A. precedens*. As currently understood, eusuchian diversity in aquatic environments during the Santonian, Campanian and Maastrichtian includes six genera: *Allodaposuchus*, *Acynodon*, *Arenysuchus*, *Iharkutosuchus*, *Massaliasuchus* and *Thoracosaurus*.

At a broader biogeographical scale, the Cretaceous European archipelago is a geographical entity. The genus *Allodaposuchus* is known exclusively from Europe and it is admittedly safe at this stage to assess that it was endemic to that area of the world. Recent work described *Pietraroiasuchus ormezzanoi* from the Albian of Italy, recognized as a member of Hylaeochampsidae (Buscalioni *et al.*, 2011). Close affinities have been recovered with *Pachycheilosuchus trinquei* from the Albian of Texas. *Pachycheilosuchus trinquei*, known from numerous postcranial elements and fragmentary cranial remains, was initially hypothesized with

close affinities to Atoposauridae (Rogers, 2003). Buscalioni *et al.* (2011) consider the North American *P. trinquei* as the only known hylaeochampsid outside Europe, which will have to be further tested with more complete skull elements of *P. trinquei*.

Originally, Vasse (1995) considered *Ischyrochampsia meridionalis* as a ‘mesosuchian’ representative, possibly a trematochampsid with Gondwanian affinities. If we consider it as a *nomen vanum* or if we refer it to *Allodaposuchus*, we observe that Late Cretaceous crocodylomorphs from Europe with a Gondwanian origin are restricted to a single taxon, *Doratodon*, with sebecosuchian affinities, a group primarily known from South America during the Cretaceous (Company *et al.*, 2005; see also Rabi & Sebök, 2014).

CONCLUSIONS

Among Late Cretaceous European eusuchians, the morphology, biogeography and phylogenetic relationships of the genus *Allodaposuchus* are attracting renewed interest. Described slightly less than a century ago on the basis of very fragmentary skull remains from Romania (Nopcsa, 1928) and then nearly forgotten for several decades, its knowledge has been recently improved thanks to the unexpected retrieval of whole and partial skulls in several localities of France, Romania and Spain (Buscalioni *et al.*, 2001; Martin & Buffetaut, 2005; Delfino *et al.*, 2008a; Ortega *et al.*, 2008; Martin, 2010; Narváez *et al.*, 2013; Puértolas-Pascual *et al.*, 2013; Blanco *et al.*, 2014). The material from the Late Campanian fluvial deposits of Velaux-La Bastide Neuve (southern France) described here represents the first chance to evaluate the variability and ontogeny of this taxon thanks to four skulls (two of which are quite complete) and a partially preserved lower jaw. The skulls share the diagnostic characters of the type species from Romania, *Allodaposuchus precedens*, and allow its diagnosis to be refined. The presence of this species in Western Europe was proposed by Buscalioni *et al.* (2001), but then questioned by Delfino *et al.* (2008a) who considered that the differences of the Spanish material could be explained by interspecific or intraspecific variation or even by different interpretations of the same morphological traits. Subsequent authors describing new materials from Spain (Puértolas-Pascual *et al.*, 2013; Blanco *et al.*, 2014) accepted the first option, considered *A. precedens* as limited to Romania, and erected the new species *Allodaposuchus subjuniperus* and *Allodaposuchus palustris*. On the basis of the variability shown by the new specimens described from the new French locality, *A. subjuniperus* is considered as valid pending confirmation but *A. palustris* is considered to lack sufficient diagnostic characters to be retained. The retrieval of further material from their type localities will hopefully clarify these issues. More-

over, on the basis of the morphology of the fragmentary dentary from Velaux-La Bastide Neuve, the first dentary associated with skull material of *Allodaposuchus* so far described, it seems likely that *Musturzabalsuchus* could be a junior synonym of *Allodaposuchus*. Also, the validity of *Ischyrochampsia meridionalis* is questionable. The result of the phylogenetic analysis that includes the coding of *A. precedens* based on the material from Velaux-La Bastide Neuve strengthens the placement of *Allodaposuchus* among the hylaeochampsid basal eusuchians.

ACKNOWLEDGMENTS

We gratefully acknowledge the management, logistical and communication assistance from the Velaux Municipality (J. P. Maggi and L. Melhi) with its heritage, culture and technical services (M. Calvier, C. Cauhape and S. Chauvet), the environment department from CG 13 (S. Amico, N. Mouly, M. Bourrelly and G. Michel), the ‘Service Départemental d’Incendie et de Secours’ (SDIS) 13 and numerous field volunteers. We also thank L. Cavin, G. Cuny and M. Feist for scientific discussions and S. Goolaerts who discovered the ‘big skull’ during the field campaigns of 2012. This work was supported by the proposals of CG 13: MAPADGAC23112010-1 and MAPADGAC16012014-1-AAPC. J.E.M. thanks R. Allain (MNHN, Paris) for access to material of *Ischyrochampsia meridionalis* and E. Frey (SMNK, Karlsruhe) for organizing his visit in the collections. M.D. was supported by Università di Torino (Fondi di Ricerca Locale 2012, 2013 and 2014) and Generalitat de Catalunya (2014 SGR 416 GRC). We thank the Editor, P. Hayward, and the Reviewers, A. Ósi and A. Hastings for their constructive comments that helped to improve the final version of this work.

REFERENCES

- Andrews CW. 1913.** On the skull and part of the skeleton of a crocodile from the Middle Purbeck of Swanage, with the description of a new species (*Pholidosaurus laevis*) and a note on the skull of *Hylaeochampsia*. *Annals and Magazine of Natural History, London* **11**: 485–494.
- Blanco A, Puértolas-Pascual E, Marmi J, Vila B, Sellés AG. 2014.** *Allodaposuchus palustris* sp. nov. from the Upper Cretaceous of Fumanya (South-Eastern Pyrenees, Iberian Peninsula): systematics, palaeoecology and palaeobiogeography of the enigmatic allodaposuchian crocodylians. *PLoS ONE* **9**: e115837.
- Brochu CA, Parris DC, Smith Grandstaff B, Denton RK, Gallagher WB. 2012.** A new species of *Borealosuchus* (Crocodyliformes, Eusuchia) from the Late Cretaceous–early Paleogene of New Jersey. *Journal of Vertebrate Paleontology* **32**: 105–116.

- Buscalioni AD, Ortega F, Vasse D. 1997.** New crocodiles (Eusuchia: Alligatoroidea) from the Upper Cretaceous of Southern Europe. *Comptes Rendus de l'Académie des Sciences de Paris* **325**: 525–530.
- Buscalioni AD, Ortega F, Vasse D. 1999.** The Upper Cretaceous crocodilian assemblage from Laño (Northcentral Spain): implications in the knowledge of the finicretaceous European faunas. *Estudios del Museo de Ciencias Naturales de Alava* **14** (Special vol. 1): 213–233.
- Buscalioni AD, Ortega F, Weishampel DB, Jianu CM. 2001.** A revision of the crocodyliform *Allodaposuchus precedens* from the Upper Cretaceous of the Hateg Basin, Romania. Its relevance in the phylogeny of Eusuchia. *Journal of Vertebrate Paleontology* **21**: 74–86.
- Buscalioni AD, Piras P, Vullo R, Signore M, Barbera C. 2011.** Early eusuchia crocodylomorpha from the vertebrate-rich Plattenkalk of Pietraroia (Lower Albian, southern Apennines, Italy). *Zoological Journal of the Linnean Society* **163**: S199–S227.
- Company J, Suberbiola XP, Ruiz-Omeñaca JI, Buscalioni AD. 2005.** A new species of *Doratodon* (Crocodyliformes: Ziphosuchia) from the Late Cretaceous of Spain. *Journal of Vertebrate Paleontology* **25**: 343–353.
- Csiki-Sava Z, Buffetaut E, Ósi A, Pereda-Suberbiola X, Brusatte SL. 2015.** Island life in the Cretaceous – faunal composition, biogeography, evolution, and extinction of land-living vertebrates on the Late Cretaceous European archipelago. *ZooKeys* **469**: 1–161.
- Csiki-Sava Z, Grigorescu D. 1998.** Small theropods from the Late Cretaceous of the Hateg Basin (Western Romania) – an unexpected diversity at the top of the food chain. *Oryctos* **1**: 87–104.
- Delfino M, Codrea V, Folie A, Dica P, Godefroit P, Smith T. 2008a.** A complete skull of *Allodaposuchus precedens* Nopcsa, 1928 (Eusuchia) and a reassessment of the morphology of the taxon based on the Romanian remains. *Journal of Vertebrate Paleontology* **28**: 111–122.
- Delfino M, Martin JE, Buffetaut E. 2008b.** A new species of *Acynodon* (Crocodylia) from the Upper Cretaceous (Santonian–Campanian) of Villaggio del Pescatore, Italy. *Palaeontology* **51**: 1091–1106.
- Delfino M, Sánchez-Villagra MR. 2010.** A survey of the rock record of reptilian ontogeny. *Seminars in Cell and Developmental Biology* **21**: 432–440.
- Dercourt J, Gaetani M, Vrielynck B, Barrier E, Biju-Duval B, Brunet M-F, Cadet J-P, Crasquin S, Sandulescu M. 2000.** *Atlas Peri-Tethys. Palaeogeographical maps*. Paris: CCGM/CGMW, 24 maps.
- García G, Fournier F, Amico S, Thouand E, Valentin X. 2010.** A new titanosaur genus (Dinosauria, Sauropoda) from the Late Cretaceous of southern France and its paleobiogeographic implications. *Bulletin de la Société Géologique* **181**: 269–277.
- García G, Vianey-Liaud M. 2001.** Dinosaur eggshells as new biochronological markers in Late Cretaceous continental deposits. *Palaeogeography, Palaeoclimatology, Palaeoecology* **169**: 153–164.
- Gmelin J. 1789.** *Linnei systema naturae*. Leipzig: G. E. Beer.
- Goloboff PA, Farris JS, Nixon K. 2003.** TNT: tree analysis using new technologies Program and documentation. Available at: <http://www.lillo.org.ar/phylogeny/tnt/>
- Gradstein F, Ogg J, Schmitz M, Ogg G. 2012.** The Geologic Time Scale 2012, 2-Volume Set (Elsevier, 2012). Amsterdam: Elsevier.
- Grigorescu D, Venczel M, Csiki Z, Limborea R. 1999.** New latest Cretaceous microvertebrate fossil assemblages from the Hateg Basin (Romania). *Geologie en Mijnbouw* **78**: 301–314.
- Huxley TH. 1875.** On *Stagonolepis robertsoni*, and on the evolution of the Crocodilia. *Quarterly Journal of the Geological Society* **31**: 423–438.
- Iordansky NN. 1973.** The skull of the Crocodylia. In: Gans C, Parson TS, eds. *Biology of the Reptilia, Vol. 1, morphology*. London: Academic Press, 201–262.
- Martin JE. 2007.** New material of the Late Cretaceous globidontan *Acynodon iberoccitanus* (Crocodylia) from southern France. *Journal of Vertebrate Paleontology* **27**: 362–372.
- Martin JE. 2010.** A new species of *Diplocynodon* (Crocodylia, Alligatoroidea) from the Late Eocene of the Massif Central, France, and the evolution of the genus in the climatic context of the Late Palaeogene. *Geological Magazine* **147**: 596–610.
- Martin JE, Buffetaut E. 2005.** An overview of the Late Cretaceous crocodilian assemblage from Cruzy, southern France. *Kaupia* **14**: 33–40.
- Martin JE, Delfino M. 2010.** Recent advances on the comprehension of the biogeography of Cretaceous European eusuchians. *Palaeogeography, Palaeoclimatology, Palaeoecology* **293**: 406–418.
- Martin JE, Rabi M, Csiki Z. 2010.** Survival of *Theriosuchus* (Mesoeucrocodylia: Atoposauridae) in a Late Cretaceous archipelago: a new species from the Maastrichtian of Romania. *Die Naturwissenschaften* **97**: 845–854.
- Martin JE, Rabi M, Csiki-Sava Z, Vasile S. 2014a.** Cranial morphology of *Theriosuchus sympiestodon* (Mesoeucrocodylia, Atoposauridae) and the widespread occurrence of *Theriosuchus* in the Late Cretaceous of Europe. *Journal of Paleontology* **88**: 444–456.
- Martin JE, Smith T, de Lapparent de Broin F, Escuillie F, Delfino M. 2014b.** Late Palaeocene eusuchian remains from Mont de Berru, France, and the origin of the alligatoroid *Diplocynodon*. *Zoological Journal of the Linnean Society* **172**: 867–891.
- Narváez I, Ortega F, Brochu C, Escaso F. 2013.** A new basal eusuchian crocodile from the Late Cretaceous of Lo Hueco (Cuenca, Spain). In: Torcida FB, Huerta P, eds. *Abstract book «VI Jornadas Internacionales sobre Paleontología de Dinosaurios y su Entorno»*. Burgos: 96–97.
- Nopcsa F. 1928.** Paleontological notes on Reptilia. 7. Classification of the Crocodilia. *Geologica Hungarica, Series Palaeontologica* **1**: 75–84.
- Ortega F, Sanz JL, Barroso-Barcenilla F, Cambra-Moo O, Escaso F, García-Oliva M, Marcos Fernández F. 2008.** El yacimiento de macrovertebrados fósiles del Cretácico Superior de 'Lo Hueco' (Fuentes, Cuenca). *Palaeontologia Nova* **8**: 119–131.

- Ósi A, Clarke JM, Weishampel DB. 2007.** First report on a new basal eusuchian crocodyliform with multicusped teeth from the Upper Cretaceous (Santonian) of Hungary. *Neues Jahrbuch für Geologie und Paläontologie Abhandlungen* **243**: 169–177.
- Prasad GV, de Lapparent de Broin F. 2002.** Late Cretaceous crocodile remains from Naskal (India): comparisons and biogeographic affinities. *Annales de Paléontologie* **88**: 19–71.
- Puértolas E, Canudo JI, Cruzado-Caballero P. 2011.** A new crocodylian from the Late Maastrichtian of Spain: implications for the initial radiation of crocodyloids. *PLoS ONE* **6**: e20011.
- Puértolas-Pascual E, Canudo JI, Moreno-Azanza M. 2013.** The eusuchian crocodylomorph *Allodaposuchus subjuniperus* sp. nov., a new species from the latest Cretaceous (upper Maastrichtian) of Spain. *Historical Biology: An International Journal of Paleobiology* **26**: 91–109.
- Rabi M, Ósi A. 2010.** Specialized basal eusuchian crocodylians in the Late Cretaceous of Europe: evidence for the hylaeochampsid affinities of *Acynodon* and its implication on alligatoroid biogeography. In 8th meeting of the European Association of Vertebrate Paleontology, Aix-en-Provence, Abstract Volume, 71.
- Rabi M, Sebők N. 2014.** A revised Eurogondwana model: Late Cretaceous notosuchian crocodyliforms and other vertebrate taxa suggest the retention of episodic faunal links between Europe and Gondwana during most of the Cretaceous. *Gondwana Research* **28**: 1197–1211. doi: 10.1016/j.gr.2014.09.015
- Riveline J. 1986.** *Les Charophytes du Paléogène et du Miocène inférieur d'Europe occidentale. Biostratigraphie des formations continentales*. Paris: Edition du CNRS.
- Rogers JV II. 2003.** *Pachycheilosuchus trinquei*, a new procoelous crocodyliform from the Lower Cretaceous (Albian) Glen Rose Formation of Texas. *Journal of Vertebrate Paleontology* **23**: 128–145.
- Sanchíz B. 1998.** Salientia. In: Wellnhofer P, ed. *Encyclopedia of paleoherpetology, part 4*. München: Verlag Dr. Friedrich Pfeil, 1–275.
- Turner A, Brochu C. 2010.** A reevaluation of the crocodyliform *Acynodon* from the Late Cretaceous of Europe. Abstract SVP Meeting: 178A.
- Valentin X, Godefroit P, Amico S, Decarreau A, Fournier F, Lauters P, Pereda-Suberbiola X, Villiers L, Garcia G. 2010.** The Velaux-Bastide Neuve locality (Upper Cretaceous, Bouches du Rhône): an example of margino-littoral ecosystem from Provence. 8th European workshop of vertebrate palaeontology, Aix, France. *Mésogée no. special*, Vol. 66, 57.
- Vasse D. 1995.** *Ischyrochampsia meridionalis* n.g. n.sp., un crocodylien d'affinité gondwanienne dans le Crétacé supérieur du sud de la France. *Neues Jahrbuch für Geologie und Paläontologie Monatshefte* **8**: 501–512.
- Webb GJW, Manolis SC, Sack GC. 1983.** *Crocodylus johnstoni* and *C. porosus* coexisting in a tidal river. *Wildlife Research* **10**: 639–650.
- Weishampel DB, Csiki Z, Benton MJ, Grigorescu D, Codrea V. 2010.** Palaeobiogeographic relationships of the Hațeg biota – between isolation and innovation. *Palaeogeography, Palaeoclimatology, Palaeoecology* **293**: 419–437.
- Wu X-C, Brinkman DB, Fox RC. 2001.** A new crocodylian (Archosauria) from the basal Paleocene of the Red Deer River Valley, southern Alberta. *Canadian Journal of Earth Science* **38**: 1689–1704.

SUPPORTING INFORMATION

Additional Supporting Information may be found in the online version of this article at the publisher's web-site:

Appendix S1. Skull measurements used in the linear regression for the analysis on the skull ontogeny of *Allodaposuchus*. Measurements of the specimens described in this study are also provided.

Appendix S2. Data matrix used for the phylogenetic analysis of the present study and including the character coding for the specimens from Velaux-Bastide-Neuve.